

Journal of Environmental Management

The spatio-temporal dynamics of suspended sediment sources based on a novel indexing approach combining Bayesian geochemical fingerprinting with physically-based modelling --Manuscript Draft--

Manuscript Number:	JEMA-D-23-07126R1
Article Type:	Research Article
Keywords:	Sediment fingerprinting, MixSIAR model, prior information, particle size distribution, INVEST model
Corresponding Author:	Renji Remesan Kharagpur, INDIA
First Author:	Arnab Das
Order of Authors:	Arnab Das Renji Remesan Adrian L. Collins Ashok Kumar Gupta
Abstract:	<p>Applications of sediment source fingerprinting continue to increase globally as the need for information to support improved management of the sediment problem persists. In our novel research, a Bayesian fingerprinting approach using MixSIAR was used with geochemical signatures, both without and with informative priors based on particle size and slope. The source estimates were compared with a newly proposed Source Sensitivity Index (SSI) and outputs from the INVEST-SDR model. MixSIAR results with informative priors indicated that agricultural and barren lands are the principal sediment sources (contributing ~5 to 85 % and ~5 to 80% respectively during two sampling periods i.e. 2018-2019 and 2021-2022) with forests being less important. The SSI spatial maps (using % clay and slope as informative priors) showed > 78% agreement with the spatial map derived using the INVEST-SDR model in terms of sub-catchment prioritization for spatial sediment source contributions. This study demonstrates the benefits of combining geochemical sediment source fingerprinting with SSI indices in larger catchments where the spatial prioritization of soil and water conservation is both challenging but warranted.</p>
Suggested Reviewers:	Gubash Azhikodan gubash@tmu.ac.jp Ilan Holman i.holman@cranfield.ac.uk Athira P athira@iitpkd.ac.in Rohini Kumar rohini.kumar@ufz.de Somsubhra Chakraborty somsubhra@agfe.iitkgp.ac.in

The spatio-temporal dynamics of suspended sediment sources based on a novel indexing approach combining Bayesian geochemical fingerprinting with physically-based modelling

Arnab Das¹, Renji Remesan^{1*}, Adrian L. Collins²,

Ashok Kumar Gupta³

¹School of Water Resources, Indian Institute of Technology Kharagpur, India

²Sustainable Agriculture Sciences, Rothamsted Research, North Wyke, Okehampton EX202SB, UK

³Department of Civil Engineering, Indian Institute of Technology Kharagpur, India

CORRESPONDING AUTHOR:

Dr. RENJI REMESAN

School of Water Resources

Indian Institute of Technology Kharagpur

Kharagpur - 721302, India

E-mail: renji.remesan@swr.iitkgp.ac.in

Tel: +91-3222-281888 (Off)

FAX: +91 3222 282212 (Off)

14th July, 2023

School of Water Resources
IIT Kharagpur
West Bengal
India

Editor – *Journal of Environmental Management*
AGU

Dear Professor Dr. Jason Michael Evans,

Research paper: The spatio-temporal dynamics of suspended sediment sources based on a novel indexing approach combining Bayesian geochemical fingerprinting with physically-based modelling.

We had two referee reports and comments from editor suggesting minor revision on this manuscript. We have carefully revised the manuscript with acute attention and utmost respect.

We have attended all comments from all two reports. Please find the revised manuscript with track changed mode and the final version along with author response to each referee comments.

We do hope that the referees and the Editor would find the revised manuscript more interesting and recommend a publication in JEMA very soon.

We look forward to hearing from you.

Yours sincerely



Dr Renji Remesan, IIT Kharagpur

Editor's comments

General Comment: Following this message are the reviews of the above-referenced manuscript. We'll be pleased to accept this paper for publication after it's been revised in accordance with the reviewers' comments. Please proofread it carefully for typographical and grammatical errors. With the revised manuscript, please provide a detailed response to the reviewers' comments, indicating how each comment is addressed in the revised manuscript. If you disagree with any of the reviewers' comments, please address them in a rebuttal.

Reply: We would like to express our gratitude for the timely and positive review reports and for an indication that you are inclined to accept our manuscript after the suggested modifications. We have diligently addressed all the review comments provided by both reviewers with great care and consideration. The significant changes made to the R1 manuscript are as follows:

- We have included a new figure, Figure 6, which presents the spatial distribution of selected elemental proportions in the soil samples, as recommended by the reviewer.
- We have made modifications to Figure 1 in accordance with the suggestions provided by both reviewers 1 and 2.
- We have thoroughly proofread the manuscript using a Grammarly premium account to ensure accuracy and clarity.
- To further improve the R1 manuscript, we have incorporated a selection of the latest references relevant to the sediment source fingerprinting topic.

Reviewer 1 comments

General Comment 1 : Reviewer #1: The research paper "The spatio-temporal dynamics of suspended sediment sources based on a novel indexing approach combining Bayesian geochemical fingerprinting with physically based modelling" by Das and co-authors, submitted to Journal of Environmental Research (JEMA-D-23-07126), combines interesting and pertinent methodological approaches to the complex interactions between of soil erosion processes - sediment source identification - sediment delivery and land use at catchment scale, an important issue for soil quality and water resource management at regional scale. Combination / comparison of physical modelling and statistical approaches of sediment fingerprinting for delivery and soil source contribution issues lead to fruitful but rather complicated investigation and outputs. Together with land use classification, slope

information and sub-catchment connectivity determinations, the study uses geochemical and textural (sediment grain size distribution) measurements to assess a source sensitivity index integrating physical and sediment source apportionment at catchment's scale. The authors also put forward some of the limitations and necessary future investigations of their study that is really of valuable assistance.

***Reply:** We would like to express our sincere gratitude for the reviewer acknowledging the relevance of our work. The authors deeply appreciate the positive comments, which endorse our novel methodological approach. We firmly believe that our proposed indexing approach, which combines the outcomes of sediment fingerprinting and physically based modelling, holds significant potential in providing valuable management insights at the catchment level.*

General Comment 2: Although commendable efforts have been made to provide a well written manuscript, this paper is rather difficult to follow for non-specialized. The relationships between "real data", i.e., direct comparison between geochemical / textural properties of sediments and source soils (1st order approach) are not displayed and the paper directly deals with outputs from data treatments (2nd order approach). Furthermore, soil source samples are made up composite aliquots at each sampling site, a procedure that likely reduces potential geochemical discrimination properties. However, the references cited by the authors aim to provide reliable support to this study's main goals and fills up the methodological gaps. Accordingly, I recommend publication of this manuscript with limited (-minor) additions / changes detailed in the following.

***Reply:** We sincerely appreciate the valuable feedback and constructive comments on our draft manuscript. We have addressed these comments in the R1 m/s as follows:*

***Point 1. Difficult to follow for non-specialized readers:** We have done minor modifications of the text and graphical abstract to ensure that key concepts and findings are presented in a concise and accessible manner to improve the manuscript's readability for non- specialised – please see ln 83-87 and 106-109 in R1 m/s.*

Line no. 83-87

“While catchment managers are interested in the interplay between areas of high risk erosion and sediment delivery, this interplay can be complex, especially in large river catchments, and the sediment fingerprinting technique is a powerful tool to enhance the

understanding of sediment contributions from different types of sources in the watershed (such as land use classes, geological units, and tributary sub-catchments).”

Line no. 106-109

“In order to better understand catchment-wide erosion and sediment delivery mechanisms, this study combines the RUSLE-based INVEST-SDR model with geochemical sediment source fingerprinting in the Konar catchment, India.”

Point 2: 2nd order approach: *As the reviewer pointed out, the manuscript does indeed focus on the outputs derived from data treatments (2nd order approach) as our primary objective was framed so. No additional content was incorporated into the R1 manuscript in connection with this as no specific alterations were suggested by the reviewer. However, we tried our best to justify this approach by citing recent studies adopting a similar methodology – please see ln 44-51 in the R1 m/s.*

Line no. 44-51

“Information on the contributions of different land use groups can be particularly informative for watershed management, and the sediment fingerprinting method based on statistically robust geochemical signatures can, in some instances, be used for obtaining such information (Demiguel et al., 2005; Laceby & Olley, 2015; Tiecher et al., 2018). To link the signatures of the sampled target sediment to the signatures of the sources, fingerprinting investigations typically combines the selected tracers (e.g., geochemical) with statistical techniques for source discrimination and numerical unmixing models for source apportionment.”

Point 3: regarding use of composite aliquots: *We understand your concern about potential reductions in geochemical discrimination while doing composite sampling. However, it is important to note that the composite sampling procedure is established internationally as part of state-of-the-art source fingerprinting procedures (see, for example, Collins et al. 2017 – Journal of Environmental Management) Adoption of the approach is necessary to account for spatial heterogeneity within the sampling sites and to ensure that sample numbers are managed in the context of study resources. We have added a few lines in the R1 manuscript to highlight these aspects. Please see **ln 146-155 in the R1 manuscript:***

Line no. 147-156

“The soil sampling plan was designed to cover the spatial heterogeneity of the land use classes in the study catchment and Google Earth and topographic data were used to locate the sampling points (Boardman, 2016). Adopting a composite sampling design is a practical solution to the issue of collecting enough source samples for statistical reliability when applying the sediment fingerprinting approach (Collins et al., 2017; Collins & Walling, 2002; Williamson et al., 2023). To execute the composite sampling approach, 105 sites distributed throughout the study catchment and representative of the different land use were used. Figure 2 shows photographs taken during the sampling campaign for both the land use source classes and for target sediment in the Konar reservoir (details of sampling protocol are shown in supplementary Table T1).”

Specific Comments

Comment 1: I suggest that the authors provide some information on the soil source composition, i.e., add a map for a selected relevant / discriminant geochemical parameter (as in Fig. 1).

Reply: Agreed and amended. As per the suggestion of the reviewer, we have added Figure 6 to show the spatial variation of elemental proportion among the soil samples collected from the 105 sampling sites. We have mainly depicted the spatial patterns of Fe, K, Ti and Ca.

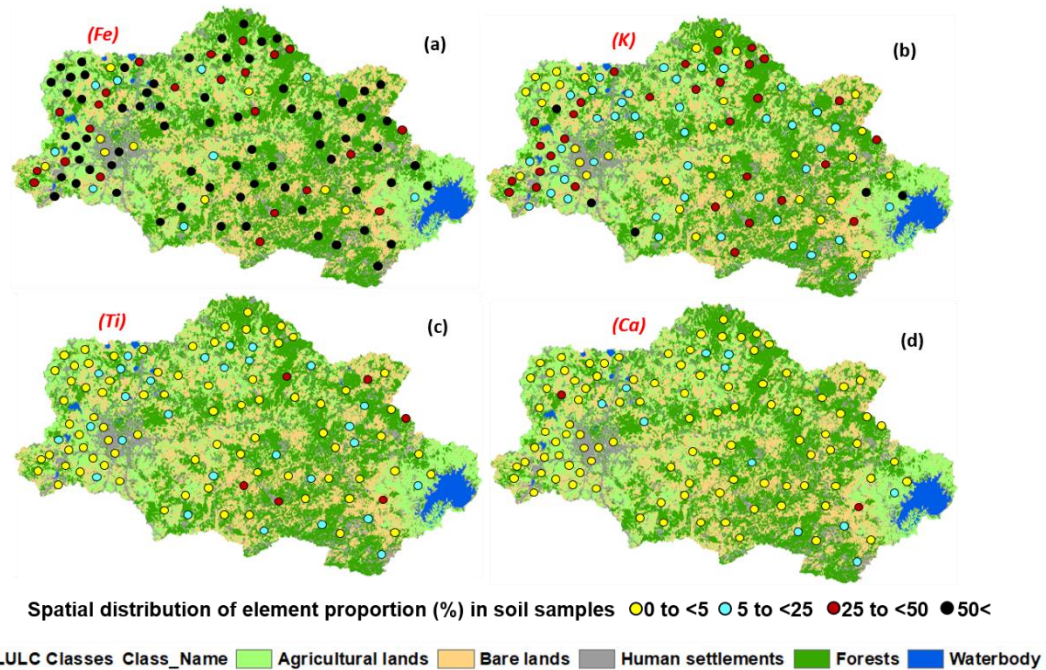


Figure 6 Spatial variation of elemental proportion (%) of (a) Fe, (b) K, (c) Ti and (d) Ca among the soil samples collected from the study catchment.

Comment 2: I also think that the authors should map the location of their 105 sample composites using one of their maps (i.e., Fig.1) so that the reader can visualize the distribution and representativeness of sampling.

Reply: Agreed and amended. As per the suggestions, we have added the sampling locations in Figure 1c (i.e., on the DEM map of the study catchment). We have also added the gauging station and the inlet of the reservoir (location of target sediment sampling).

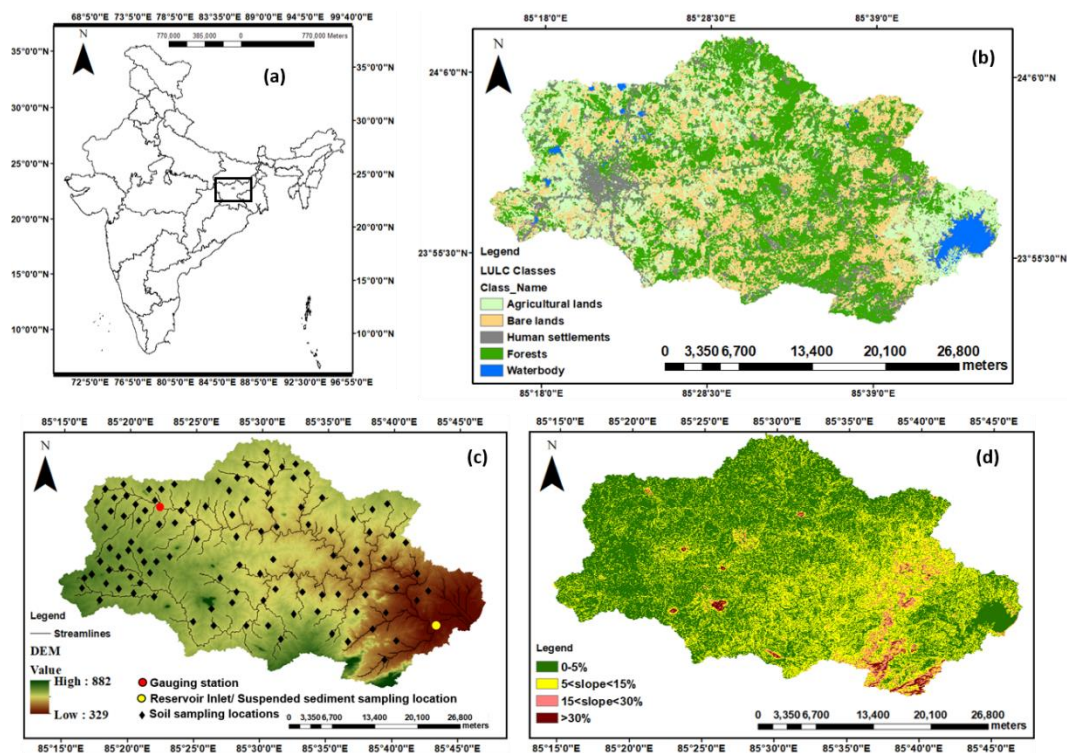


Figure 1. Information on the Konar study catchment characteristics: (a) location (b) land use (c) DEM (d) slope.

Comment 3: Are the results of this study (i.e., sediment export and export rates, section 3.4) supported by other nearby environments?

Reply: Yes, the results of this study are in good agreement with the few other studies performed in this catchment. Specifically, one of our previous soil erosion and sediment yield studies (Das et al., 2022) conducted on this catchment, and the outcomes of the sediment fingerprinting results are in good agreement in identifying the crucial land use classes of the catchment. The mean annual sediment export identified in this study is computed to be 11 tons/unit area as compared to 10 tons/ha/year for agricultural areas and ~25 tons/ha/year reported by Das et al., (2022) and Rajbanshi & Bhattacharya, (2020) respectively. We have

discussed this aspect in the discussion section in the R1 m/s. Please refer to **ln 345-357** in the R1 m/s:

Line no. 345-357

“The highest human settlement contribution was estimated using the P0 model. However, the P0 model underestimated the contribution of barren lands drastically, and this land use has been reported to be a major sediment source by other studies (Das et al., 2022; Rajbanshi & Bhattacharya, 2020). The clay prior (P1) based model identified barren lands as the major sediment source (~20 to 70%) followed by agricultural lands (~10 to 70%) during both timeframes. Similar source estimates were generated using the slope based prior (P4) model. This suggests that the steepness of slope in the barren land areas is a major factor controlling sediment sources in the study catchment (Mishra et al., 2022). The silt based prior model (P2) predicted similar source contributions to the P0 model by identifying agricultural lands and human settlement areas as major sediment sources. The effects of silt concentration on geochemical properties were found to be negligible by Kraushaar et al., (2015) and this explains the lack of any significant difference between the source estimates using the silt based prior and no prior (P0) models.”

The full reference details for the additional reference is now on **ln 353** in the R1 m/s.

Rajbanshi, J., & Bhattacharya, S. (2022). Modelling the impact of climate change on soil erosion and sediment yield: A case study in a sub-tropical catchment, India. Modeling Earth Systems and Environment, 8(1), 689–711. <https://doi.org/10.1007/s40808-021-01117-4>

Minor comments

Most of my other "minor" requests refer to the "2. methodology section".

Comment 4: Soil and sediment preparation: I understand that samples were dry sieved at 63 µm after oven drying. Therefore, sieving involved aggregates of soil particles during drying. How the authors assume that there <63 µm size fractions were accurately separated? Sample preparation usually requires wet sieving and some preliminary "soft" grinding (to avoid overgrinding). Some precision is needed.

Reply: We appreciate your insightful comment regarding the soil and sediment preparation in our study. However, we did take measures to minimize aggregation effects during the dry sieving process. To obtain the proportion of <63 µm particles in the soil samples we oven

dried them for nearly 12 hrs and the soil samples were passed through a 63 μm sieve shaker for 24 hours. We also ensured that the sieving equipment used was of high quality with precise mesh sizes with prolonged oven drying and extended sieving duration to enhance the separation process. While wet sieving and preliminary grinding can be effective in certain contexts, we didn't adopt those in our study. We plan to consider trade-offs between different sampling and processing methods in future research.

Moreover, we conducted particle size analysis on the soil samples to generate prior distributions for Bayesian modelling, and the results exhibited a substantial level of concordance with the proportion of fine soil particles that were extracted from the soil samples.

Comment 5: "the" instead of "he" in the figure legend

Reply: *Agreed and amended.*

Comment 6: Fig. 10: please improve horizontal and vertical scales by adding intermediate graduations

Reply: *Agreed and amended.*

Comment 7: Reference list:

Reply: *Agreed and amended.*

- *Burrough Jr... incomplete: Removed*
- *Palazon... duplicates: Modified accordingly*
- *Upadhhayay... duplicates: Modified accordingly*
- *Small et al... incomplete: Modified accordingly*
- *Stock et al... incomplete: Modified accordingly*

Specific Comments

General Comment: The manuscript Number: JEMA-D-23-07126 entitled "The spatio-temporal dynamics of suspended sediment sources based on a novel indexing approach combining Bayesian geochemical fingerprinting with physically based modelling" is well written. On the other hand, there are some essential comments authors should take into consideration.

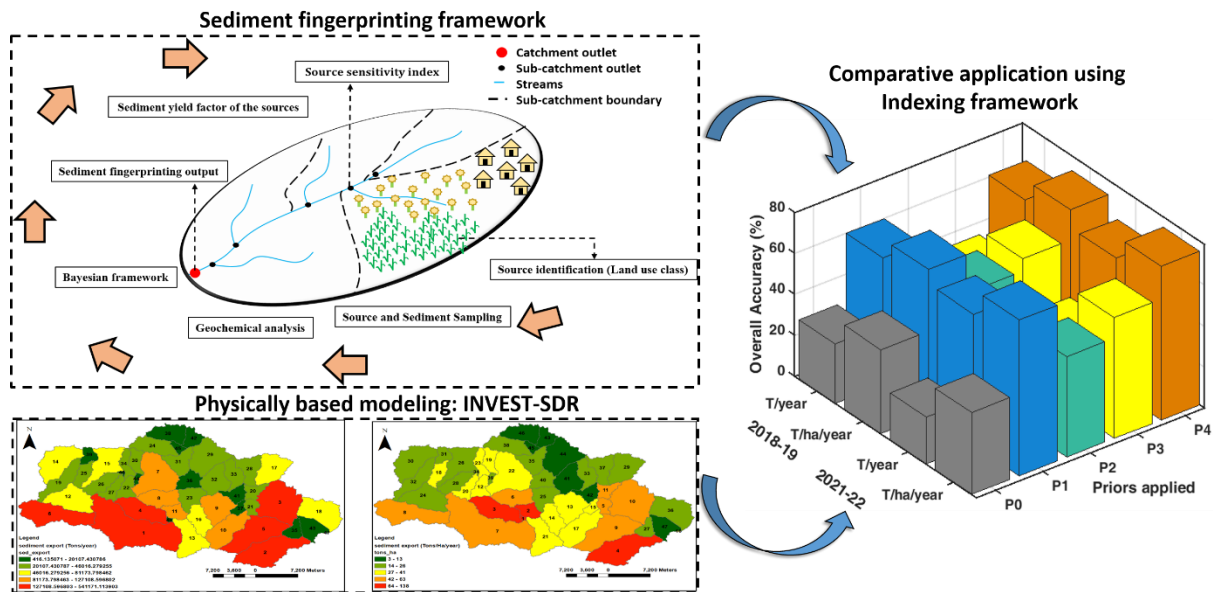
Reply: *We express our sincere gratitude to the reviewer for their favourable assessment of the novel methodology we employed for sediment fingerprinting. The integration of the indexing method and physically based modelling has provided valuable insights into the potential sediment production within our catchment. We have diligently addressed all the reviewer's comments in the subsequent responses, ensuring their inclusion in our R1 manuscript.*

Reviewer 2 Comments

Comment 1: Graphical abstract does not provide the visual interpretations of the manuscript.

Reply: *Agreed and amended.* As per the recommendation, we have modified the graphical abstract to make it a more precise and proper representation of the work. Please see the following figure:

Graphical abstract



Comment 2: More recent studies can be referred in the literature review.

Reply: *Agreed and amended.* As per the comment, we have updated the R1 manuscript by citing the following recent references for sediment source fingerprinting work:

Hirave, P., Nelson, D. B., Glendell, M., & Alewell, C. (2023). Land-use-based freshwater sediment source fingerprinting using hydrogen isotope compositions of long-chain fatty acids. *Science of The Total Environment*, 875, 162638.

<https://doi.org/10.1016/j.scitotenv.2023.162638> - - see ln 71 in the R1 m/s

Lake, N. F., Martínez-Carreras, N., Iffly, J. F., Shaw, P. J., & Collins, A. L. (2023). Use of a submersible spectrophotometer probe to fingerprint spatial suspended sediment sources at catchment scale. *Science of The Total Environment*, 873, 162332.

<https://doi.org/10.1016/j.scitotenv.2023.162332> - - see ln 43 in the R1 m/s

Liu, Y., Walling, D. E., Yang, M., & Zhang, F. (2023). Sediment source fingerprinting and the temporal variability of source contributions. *Journal of Environmental Management*, 338, 117835. <https://doi.org/10.1016/j.jenvman.2023.117835> - - see ln 214 in the R1 m/s

Williamson, T. N., Fitzpatrick, F. A., & Kreiling, R. M. (2023). Building a library of source samples for sediment fingerprinting – Potential and proof of concept. *Journal of Environmental Management*, 333, 117254. <https://doi.org/10.1016/j.jenvman.2023.117254> - - see ln 152 in the R1 m/s

Xu, Z., Belmont, P., Brahney, J., & Gellis, A. C. (2022). Sediment source fingerprinting as an aid to large-scale landscape conservation and restoration: A review for the Mississippi River Basin. *Journal of Environmental Management*, 324, 116260. <https://doi.org/10.1016/j.jenvman.2022.116260> - - see ln 64 in the R1 m/s

Comment 3: Figure 1 needs a minor editing. The miles should be lower case Regarding this I would comment that the way of depicting units is incorrect.

According to the Bureau Internationale des Poids et des Mesures ' guidance, (<https://www.bipm.org/documents/20126/41483022/SI-Brochure-9.pdf/fcf090b2-04e6-88cc-1149-c3e029ad8232>) from the SI Brochure (PDF; see p. 147 for English) clause 5.2: They are printed in lower-case letters unless they are derived from a proper name, in which case the first letter is a capital letter. Few maps have the scale in miles while few are written in metres. Please check.

Reply: Agreed and amended. As per the suggestions, we have modified all the maps by updating the scale formats. We have adapted 'Meters' to 'meters' in the scale.

Comment 4: Proofreading at many places should be done. The paper needs to be thoroughly revised, and proper English writing skills should be applied.

Reply: Agreed and amended. As per the suggestion, we have undertaken proofreading using a premium Grammarly account to correct any typographical and grammatical errors.

Highlights

- Sensitivity of Bayesian sediment fingerprinting to particle size and slope explored
- Proposed a novel method to translate fingerprinting outputs to spatial information
- Method combines INVEST-SDR catchment modelling and Bayesian fingerprinting
- Combined approach revealed agricultural and barren regions as crucial sediment sources

1
2
3
4
5
6
7
8
9
10
11
12
13
14
15
16
17
18
19
20
21
22
23
24
25
26
27
28
29
30

**The spatio-temporal dynamics of suspended sediment sources based on a novel indexing
approach combining Bayesian geochemical fingerprinting with physically-based
modelling**

31
32
33
34
35
36
37
38
39
40
41
42
43
44
45
46
47
48
49
50
51
52
53
54
55
56
57
58
59
60
61
62
63
64
65

Arnab Das¹, Renji Remesan^{1*}, Adrian L. Collins²,

Ashok Kumar Gupta³

¹School of Water Resources, Indian Institute of Technology Kharagpur, India

²Net Zero and Resilient Farming, Rothamsted Research, North Wyke, Okehampton
EX202SB, UK

³Department of Civil Engineering, Indian Institute of Technology Kharagpur, India

CORRESPONDING AUTHOR:

Dr. RENJI REMESAN

School of Water Resources

Indian Institute of Technology Kharagpur

Kharagpur - 721302, India

E-mail: renji.remesan@swr.iitkgp.ac.in

Tel: +91-3222-281888 (Off)

FAX: +91 3222 282212 (Off)

1 **Abstract**

2 Applications of sediment source fingerprinting continue to increase globally as the need for
3 information to support improved management of the sediment problem persists. In our novel
4 research, a Bayesian fingerprinting approach using MixSIAR was used with geochemical
5 signatures, both without and with informative priors based on particle size and slope. The
6 source estimates were compared with a newly proposed Source Sensitivity Index (SSI) and
7 outputs from the INVEST-SDR model. MixSIAR results with informative priors indicated that
8 agricultural and barren lands are the principal sediment sources (contributing ~5 to 85 % and
9 ~5 to 80% respectively during two sampling periods i.e. 2018-2019 and 2021-2022) with
10 forests being less important. The SSI spatial maps (using % clay and slope as informative
11 priors) showed > 78% agreement with the spatial map derived using the INVEST-SDR model
12 in terms of sub-catchment prioritization for spatial sediment source contributions. This study
13 demonstrates the benefits of combining geochemical sediment source fingerprinting with SSI
14 indices in larger catchments where the spatial prioritization of soil and water conservation is
15 both challenging but warranted.

16 **Keywords:** Sediment fingerprinting, MixSIAR model, prior information, particle size
17 distribution, INVEST model

27

28 **1. Introduction**

29 Water erosion is regarded as the most serious concern to global soil security, resulting in poorer
30 agriculture yields and pollution of freshwater resources and estuaries (Das et al., 2022). A
31 significant amount of research and policy attention is still directed towards reducing
32 reservoir siltation and water pollution caused by water erosion; most notably, excess fine-
33 grained ($< 63 \mu\text{m}$) sediment (Collins et al., 2020). Understanding water-induced soil erosion,
34 sediment delivery and export, and sediment source patterns is crucial for targeted management
35 of the impacts of human actions and natural processes on soil health and water resources.
36 Though erosion models can be used for screening likely erodible areas in a catchment, critical
37 information on sediment provenance can be obtained using sediment source fingerprinting
38 (Lizaga et al., 2022). In particular, it is useful to identify the areas with disproportionately high
39 erosion rates and connectivity with river channels, for developing optimal management
40 strategies (Abban et al., 2016).

41 Several investigations have determined the relative contributions of surface and
42 instream sources to sediment loads (Afshar et al., 2016; Boudreault et al., 2019; Carter et al.,
43 2003; Collins & Walling, 2002, 2007; Lake et al., 2023). Geochemical fingerprinting of
44 sediments is one of the most widely used approaches (Collins et al., 2020). Information on the
45 contributions of different land use groups can be particularly informative for watershed
46 management, and the sediment fingerprinting method based on statistically robust geochemical
47 signatures can, in some instances, be used for obtaining such information (Demiguel et al.,
48 2005; Laceby & Olley, 2015; Tiecher et al., 2018). To link the signatures of the sampled target
49 sediment to the signatures of the sources, fingerprinting investigations typically combines the
50 selected tracers (e.g., geochemical) with statistical techniques for source discrimination and
51 numerical unmixing models for source apportionment. Various unmixing models have been

1
2
3
4
5
6
7
8
9
10
11
12
13
14
15
16
17
18
19
20
21
22
23
24
25
26
27
28
29
30
31
32
33
34
35
36
37
38
39
40
41
42
43
44
45
46
47
48
49
50
51
52
53
54
55
56
57
58
59
60
61
62
63
64
65
66
67
68
69
70
71
72
73
74
75
76
77
78
79
80
81
82
83
84
85
86
87
88
89
90
91
92
93
94
95
96
97
98
99
100

proposed and used, including frequentist and Bayesian approaches (Collins, 2020; Collins et al., 2017; Davis & Fox, 2009; D’Haen et al., 2013). In order to determine the sources of target sediment, the Bayesian approach combines the likelihood of current sediment source data (geochemistry) with prior knowledge of sediment sources to form a posterior probability distribution of source contributions (Small et al., 2002). The assumption that tracers are adequately characterized for the potential source areas and the target sediment samples is eased when previous information is used for model parameterisation (Billheimer, 2001). Here, it is regarded by some investigators that Bayesian approaches are best for illustrating the uncertainty associated with estimated sediment source contributions.

Complex landscapes, however, make it difficult to pinpoint the origins of fine-grained sediment. As a result, new methods are required to provide additional insights into the interplay between catchment structure, surface cover, and land use practices for determining sediment source contributions (Tang et al., 2019; Xu et al., 2022). In support of this, Bayesian unmixing model frameworks can include prior information for relevant catchment characteristics (Stock et al., 2018; Upadhayay et al., 2017). In the existing literature, numerous possibilities are discussed concerning the applicability of prior information in Bayesian frameworks for understanding sediment dynamics at catchment scale. A study by Upadhayay et al., (2020), for example, applied a sediment connectivity index as prior information to identify the crucial land use classes of a study catchment. Similar attempts have also been made by other studies by using other catchment information such as land cover area (Hirave et al., 2023; Lizaga, 2021; Upadhayay et al., 2017, 2022). Beyond connectivity or land cover associated risks for erosion and sediment delivery, the effect of particle size selectivity on sediment source signals is widely recognised in many previous studies (Haddadchi et al., 2015; Gaspar et al., 2022). When it comes to rain-induced erosion, raindrops and slope controls the detachment and delivery of soil particles (Lu et al., 2016). In particular, the particle size distributions of sediment are useful

1
2
3
4
5
6
77 background knowledge for elucidating soil erosion processes (Legout et al., 2005; Cheraghi et
8
9
10
11
12
13
14
15
16
17
18
19
20
21
22
23
24
25
26
27
28
29
30
31
32
33
34
35
36
37
38
39
40
41
42
43
44
45
46
47
48
49
50
51
52
53
54
55
56
57
58
59
60
61
62
63
64
65

78 al., 2016; Kiani-Harchegani et al., 2019), making such understanding an effective form of prior
79 information.

80 Despite the aforementioned importance of specific catchment characteristics, source
81 apportionment studies have not, to date, explored the sensitivity of the results to the
82 combination of mean slope and particle size.

83 While catchment managers are interested in the interplay between areas of high risk erosion
84 and sediment delivery, this interplay can be complex, especially in large river catchments, and
85 the sediment fingerprinting technique is a powerful tool to enhance the understanding of
86 sediment contributions from different types of sources in the watershed (such as land use
87 classes, geological units, and tributary sub-catchments). Here, combining sediment
88 fingerprinting methods with physical erosion modelling and other indices has been shown to
89 improve the efficacy of management decisions [e.g. (Palazón et al., 2014, 2016; Wilkinson et
90 al., 2013)]. By combining the application of physically-based modelling and sediment
91 fingerprinting methods at the catchment scale, it is possible to create novel indicators of the
92 spatio-temporal variability of sediment sources [i.e. source sensitivity index (SSI)]. Previous
93 studies have, for instance, shown the value of combining weathering indices with conventional
94 geochemical tracers to gain further insight into sub-basin spatial suspended sediment sources
95 (Nosrati et al., 2019). Integrating indices with sediment fingerprinting results can help to: (i)
96 elucidate sub-catchment scale erosion processes spatially, (ii) improve the accuracy of
97 sediment source fingerprinting, and; (iii) support comparisons between sediment fingerprinting
98 results and physical modelling outputs as a weight-of-evidence approach to understanding
99 catchment sediment dynamics. Developing SSI can address sampling uncertainties and the
100 spatial limitations frequently associated with sediment fingerprinting results (Collins, 2020;
101 Collins et al., 2017; Koiter et al., 2013). Previous research using the SWAT model has shown

102 that the integration of physical modelling and tracer-based methods on large river systems
103 greatly improves our understanding of erosion processes (Palazón et al., 2014, 2016; Wilk,
104 2022). Similar to the SWAT model, the INVEST-SDR model has been extensively applied to
105 deal with a wide range of scales and issues related to sediment delivery modelling across
106 various hydro climatic regions (Hamel et al., 2017; Vigerstol & Aukema, 2011). In order to
107 better understand catchment-wide erosion and sediment delivery mechanisms, this study
108 combines the RUSLE-based INVEST-SDR model with geochemical sediment source
109 fingerprinting in the Konar catchment, India.

110 The specific objectives were:

- 111 a. To apply geochemical fingerprinting to apportion suspended sediment sources in the
112 form of land use classes.
- 113 b. To apply a Bayesian mixing model with particle size distribution and mean slope as
114 prior information and to examine the sensitivity of source apportionment estimates to
115 such data.
- 116 c. To develop an innovative index (SSI) using the geochemical fingerprinting results to
117 generate spatio-temporal soil erosion maps.
- 118 d. To assess and quantify the spatial distribution of sediment sources in the study
119 catchment using the INVEST-SDR model and compare the outputs with the sediment
120 fingerprinting and SSI results to evaluate the accuracy of the Bayesian sediment
121 fingerprinting method.

122 **2 Methodology**

123 *2.1 Study area characteristics*

124 This study was carried out in eastern India's Konar catchment (990 km²) of the Damodar River
125 basin. The Konar catchment has diverse geo-physical terrains including high plains,
126 moderate hills, and valleys. Elevations range between 329-882 m, with an eastern slope (Figure

127 1c). The climate is subtropical, with annual average rainfall of 1100-1300 mm distributed
128 mostly (70-80%) between June and September. Summer temperatures can reach 46°C
129 compared with lows of 4°C in the winter. The Hazaribagh district comprises more than 70
130 percent of the catchment area, and most of this territory is made up of forests and rocky soils.
131 Overall, our land use categories are found in the study catchment: i.e., agricultural lands (38%),
132 forests (36%), barren lands (14%), and human settlements (12%) (Figure 1b). Rice, groundnuts,
133 and maize are the primary crops cultivated in the agricultural areas during the monsoon season,
134 while wheat, mustard, and other vegetables are grown using terrace farming on uneven terrain
135 during the off-monsoon season. Mixed deciduous and tropical dry forests predominate in the
136 forest zones with several species of medicinal plants and timber trees including sal (*Shorea*
137 *robust*) (Forest, Environment and Climate change Department, Government of Jharkhand;
138 <https://forest.jharkhand.gov.in>). The three most common soil types are lithosols (46%), ferric
139 luvisols (38%), and eutric nitosols (16%) (Supplementary Figure F1).

140 ***2.2 Soil and sediment sampling***

141 One of the main challenges of the sediment fingerprinting approach is collecting sufficient
142 source samples for statistical reliability (Collins & Walling, 2002). To study the temporal
143 variation in the suspended sediment contributions from different sources, water samples were
144 collected for six time periods from the inlet of Konar reservoir (shown in Figure 1c) for two
145 alternate water years; i.e., July 2018-June 2019 and July 2021-June 2022. Three 2L swabs of
146 suspended sediment were collected at a water depth of 0-10 cm and stored in high-density
147 polyethylene bottles during these sampling periods (Wang et al., 2019). The soil sampling plan
148 was designed to cover the spatial heterogeneity of the land use classes in the study catchment
149 and Google Earth and topographic data were used to locate the sampling points (Boardman,
150 2016). Adopting a composite sampling design is a practical solution to the issue of collecting
151 enough source samples for statistical reliability when applying the sediment fingerprinting

152 approach (Collins et al., 2017; Collins & Walling, 2002; Williamson et al., 2023). To execute
153 the composite sampling approach, 105 sites distributed throughout the study catchment and
154 representative of the different land use were used. Figure 2 shows photographs taken during
155 the sampling campaign for both the land use source classes and for target sediment in the Konar
156 reservoir (details of sampling protocol are shown in supplementary Table T1). Composite
157 sampling involved merging three to four sub-samples collected within a radius of 100 to 500
158 m, depending on accessibility (Collins et al., 2017). The upper 5 cm of soil was sampled at
159 each source sampling location using a non-metallic trowel deployed in one extensive campaign.
160 This one-off source sampling strategy assumed that lithological features remained constant
161 through time (Tiecher et al., 2017).

162 ***2.3 Sample preparation and laboratory analysis***

163 To extract suspended sediments from the bulk water samples, the samples were first
164 centrifuged, then filtered, and finally oven dried at 70 °C for 12 hours. After 12 hours of oven
165 drying, soil samples were passed through a 63 µm sieve shaker for 24 hours to avoid
166 aggregation and extract the silt and clay fractions to improve the direct comparability of source
167 and sediment samples (Collins & Walling, 2016). Prior to the sample processing, scanning of
168 the soil and sediment samples was performed using a DP-6000 Delta Premium portable X-ray
169 fluorescence (PXRF) machine equipped with an Rh X-ray tube operating at 15-40 keV. Using
170 the instrument's Geochem Mode, the concentrations of V, Cr, Fe, Co, Ni, Cu, Zn, W, Hg, As,
171 Se, Pb, Bi, Rb, U, Sr, Y, Zr, Th, Mo, Ag, Cd, Sn, Sb, Ti, Mn, Mg, Al, Si, P, S, Cl, K, and Ca
172 were estimated (Sharma et al., 2014). The particle size characteristics of the source and target
173 sediment samples were measured using a Malvern Pananalytical Mastersizer 3000.

174 ***2.4 Formulation of the Bayesian framework and priors for source***

175 ***apportionment modelling***

176 Geochemical tracers were selected using a standard two-step process consisting of a Kruskal-
177 Wallis H-test for inter-group differences, and a stepwise discriminant function analysis (DFA)
178 for selecting a minimal set of tracers that maximises source discrimination (Collins et al.,
179 1997). MixSIAR, a state-of-the-art Bayesian Isotope Mixing Model (BIMM) available as a free
180 R package, was used to estimate sediment source apportionment (Guerrero & Rogers, 2020;
181 Stock et al., 2018). The geochemical tracers were entered into a concentration-dependent
182 MixSIAR model with and without the use of the informative priors (Upadhayay et al., 2020).
183 The following settings were applied for the Markov Chain Monte Carlo (MCMC) iterations:
184 number of chains = 3, chain length = 3,000,000, burn = 1,500,000, thin =500. Gelman-Rubin
185 and Geweke diagnostic statistics were used to verify model run convergence (Stock et al.,
186 2018). The deviance information criteria (DIC) was used to choose the best fitting model.
187 Means and 95% Bayesian confidence intervals (CI) were provided from posterior distributions
188 derived for sediment source contributions to estimate these contributions and their associated
189 uncertainty (Upadhayay et al., 2020). Upadhayay et al., (2017) provide a comprehensive
190 description of MixSIAR, and Stock et al., (2018) provides a comprehensive mathematical
191 explanation of MixSIAR.

2.4.1 *Prior selection*

193 Informative priors for sediment source proportions should be selected logically with proper
194 physical meaning (Upadhayay et al., 2020). Research suggests that rainfall-induced soil erosion
195 occurs in primarily three phases, each of which is particle size-based (Figure 3) (Sadeghi et al.,
196 2017; Wang & Shi, 2015). The initial stage comprises the detachment of soil particles by
197 raindrop splash - eroding mostly very fine particles and some fine particles (Figure3a). The
198 second stage i.e. after a prolonged rainfall event, is characterized by an increased proportion of
199 coarser particles and fine particles (Figure 3b). Finally, in the third stage, sediment
200 transportation of very fine particles and lower quantities of fine and coarse particles takes place

201 through the stream network (Figure 3c). The slope of the terrain plays a very important role in
 202 the erosion process (Reza Vaezi et al., 2020). In this study we explored the sensitivity of the
 203 source proportion estimates to the choice of particle size priors (clay <2 µm, silt 2-50 µm, and
 204 fine sand >50 µm) by adjusting the prior specification and observing the impacts on the
 205 posterior distributions generated by MixSIAR. Particle size priors were derived by determining
 206 the mean proportions of clay, silt, and very fine sand in the individual land use classes. Mean
 207 slopes of the land use groups were used to incorporate the slope priors.

2.5 Formulation of the source sensitivity index (SSI)

209 The sediment fingerprinting outputs provided by MixSIAR are relative and thereby do not
 210 provide information on the sediment yields from individual sources. To address this
 211 shortcoming, we developed an SSI using: (i) sediment yield factor for each land use class; (ii)
 212 proportion of area covered by each land use class in the overall catchment and the sub-
 213 catchments therein, and; (iii) information on the temporal variability of the source contribution
 214 obtained from the sediment fingerprinting analysis (Liu et al., 2023). An SSI value may be
 215 derived to show the severity of the sub-catchments by linking the area covered by the sub-
 216 catchment, the land use distribution within the sub-catchment, and the temporal variations in
 217 the total catchment's sediment production. Accordingly, the SSI was estimated as:

$$S_{ef} = \frac{X_e}{A_e} \quad (e = 1:m, f = 1:n) \quad (1)$$

$$SSI_x = \left(\sum_{f=1}^n \sum_{e=1}^m \frac{S_{ef} \cdot A_{ex}}{A_x} \right) \cdot D_x \cdot P_f \quad (2)$$

S_{ef} = sediment yield factor for land use e in the month f .

X_e = Source contribution (land use) to the catchment sediment yield obtained from the fingerprinting approach.

A_e = Area covered by respective land use class (e) in the catchment.

225 **SSI_x** = Source sensitivity of sub-catchment **x**.

226 **A_{ex}** = Area covered by land use class **e** in sub-catchment **x**.

227 **A_x** = Area covered by sub-catchment **x**.

228 **D_x** = Distance factor of the sub-catchment outlet (calculated as the ratio of longest flow path
229 and distance of the sub-catchment outlet from the catchment sink where the target sediment
230 samples were collected) (Supplementary Figure F2).

231 **P_f** = Proportion of annual sediment yield in the respective month.

232 Figure 4 depicts the analytical framework used to generate spatial maps based on SSI values in
233 our study area. This figure also shows the whole methodology of this study employing physical
234 modelling outputs to authenticate sediment fingerprinting outcomes through SSI generated
235 spatial maps.

236 ***2.6 RUSLE-based hydrological model development: INVEST-SDR***

237 Quantification and mapping of soil loss and sediment delivery in a landscape can
238 be accomplished using the Integrated Valuation of Ecosystem Services and Tradeoffs
239 (INVEST)- Sediment Delivery Ratio (SDR) model (Aneseyee et al., 2020). Compared to other
240 models, such as SWAT, INVEST-SDR uses less input data (Table 1) and is more flexible; it can
241 also be modified to a given scenario and used with locally and globally accessible data and
242 exemplifies the hydrological connectivity concept proposed by Vigiak et al., (2012). To
243 validate the INVEST SDR model, annual simulated sediment inflow data was compared to real
244 data collected from Damodar Valley Corporation (DVC) using root mean square error (RMSE)
245 and the coefficient of determination (R^2).

246

247 **3 Results**

248 ***3.1 Catchment sediment sources using geochemical source fingerprinting***

249 Correct and reliable use of sediment fingerprinting requires statistical analysis and
1
2
3 250 interpretation of isotope tracers from sediment source end members. One of the most important
4
5 251 step is to identify a representative set of final geochemical tracers to use in a "composite
6
7 252 signature" to determine the origin of fine sediments. From the laboratory analysis, 24 elements
8
9 253 were detected in the soil and sediment samples collected from the Konar catchment. To identify
10
11 254 the set of discriminatory geochemical tracers to be used as an input to the MixSIAR, all the
12
13 255 elements were passed through a KW test followed by DFA (Figure 5). Based on this analysis,
14
15 256 21 elements were selected (Fe, K, Ti, Ca, Zn, Mn, Ba, Zr, Rb, V, Cr, Sn, Ni, Sr, Pb, Cu, Ga,
16
17 257 Sb, Ag, A, and Br). A summary of the statistical analysis for source discrimination is provided
18
19 258 in supplementary Table T2. Furthermore, we have also shown the spatial variability of the
20
21 259 proportional (%) presence of few elements (Fe, K, Ti and Ca) in the soil samples collected from
22
23 260 105 locations of the catchment (Figure 6).

261 ***3.2 Bayesian modelling results for source apportionment***

262 MixSIAR was run with both 'no priors (P0)' and priors based on particle size and slope
263 information for the study catchment (details of P1 to P4 are given in Table 2). During both time
264 periods, both agricultural and barren lands were the most important sediment sources (Figure
265 7). The Bayesian model with no priors (P0) and with the silt based prior (P2) identified
266 agricultural lands as the major sediment source in most of the seasons (varying from ~30-45%
267 during the water year 2018-19 and ~30 to 60 % during the water year 2021-22) (Figure 7 a1,
268 a2). In contrast to the other prior-based models, these two models (P0 and P2) predicted a
269 smaller contribution of suspended sediment from agricultural areas and a larger contribution
270 from human settlements (Figure 7 b₁, b₂). The clay based prior (P1) and the slope based prior
271 (P4) model outputs, both identified barren lands as the primary source of suspended sediment
272 (varying from ~25-75% during the water year 2018-19 and ~20 to 60 % during water year
273 2021-22). In contrast, the outputs of the slope based prior model suggested negligible

274 contributions from human settlement areas compared with the other land use classes (varying
275 between 0-5% for both water years 2018-19 and 2021-22). The very fine sand prior (P3) based
276 model predicted a much higher contribution from forests (varying from ~20-50% during the
277 water year 2018-19 and ~25-50% during 2021-22). Overall, all the prior based models
278 identified agricultural land as the primary source of sediment in July 2021 (Figure 7 a2).

3.3 SSI based Bayesian modelling results for source apportionment

280 This study investigated the potential utility of a new index [Source Sensitivity Index (SSI)] to
281 help the policymakers better understand the relative impacts of sediment sources in the Konar
282 catchment. It integrates sediment fingerprinting information with the physical controls of
283 sediment deposition in the sub-catchments to generate an index value for ranking the sub-
284 catchments to explain conservation urgency. To establish a link with physical modelling results,
285 the sub-catchments were classified into five SSI classes [class1 (26-174), class2 (175-378),
286 class3 (379-822), class4 (823-1267), class5 (1268-5266)] (Figure 8). Figure 9 displays the
287 distribution of the sub-catchments across the SSI classes for the particle size and slope prior
288 based model outputs, suggesting little disparity among the sub-catchments using the P0 and P2
289 priors based models. However, upon closer inspection, it can be seen that the number of sub-
290 catchments with higher SSI classes is marginally greater during 2021–2022, compared with
291 2018–2019. This SSI based information and associated maps can be used for assessing the
292 reliability of mixing model source apportionment results based on the comparison with
293 physically-based model outputs. More sub-catchments under class 5 (C5) were discovered by
294 P1 based model in both time frames, similar to the P4 based model. However, it is evident from
295 the Bayesian model findings described in section 3.2 that a comparable number of sub-
296 catchments come under the prior-based models P0 and P2. Importantly, the SSI based analysis
297 demonstrated how effectively Bayesian sediment fingerprinting results can be converted into
298 translating tool to spatially explain the sediment dynamics in the Konar catchment. This SSI

299 based information and maps can be used as a criterion for assessing the reliability of mixing
300 model source apportionment results in comparison with physically based sedimentation models
301 spatial outputs.

302 ***3.4 INVEST-SDR model based results***

303 The assessment of sediment export using INVEST-SDR model involved computing the annual
304 soil loss, sediment connectivity, and sediment delivery ratio of the study catchment. According
305 to the coefficient of determination (R^2) and root mean square error (RMSE) values of 0.81 and
306 6.85 t/ha/year for the Nagwan gauging station, the predicted sediment export from the
307 catchment was in line with the available observed data over time (Supplementary Figure F3).
308 Using the sediment connectivity index (SCI) proposed by Borselli et al., (2008) the mean
309 sediment connectivity is estimated to be -6.326, ranging between -11.038 and 0.179 (Figure
310 10a). INVEST-SDR's estimate for soil loss ranged from 0 to 23321 t/year, with a mean soil loss
311 rate of 23.65 tonnes per year (Figure 10b). The sediment delivery ratio was computed based on
312 the connectivity index and ranged from 0 to 0.322, with a corresponding mean value of 0.082
313 (Figure 10c). The spatial variation in the Konar catchment's sediment export, ranging from 0
314 to 3490 t/year with a mean value of 11.16 t/year, is shown in Figure 10d. The Konar catchment
315 was sub-divided into 47 sub-catchments to pinpoint the crucial hot spots of soil erosion for
316 targeting preventative measures. All sub-catchments were ranked and classified based on the
317 sediment export in t/year (Figure 10e) and t/ha/year (Figure 10f). Here, we used two different
318 sub-catchment ranking methods. Firstly, the sub-catchments were ranked according to their
319 annual sediment yield, and secondly, the sub-catchments were ranked according to annual
320 sediment yield per unit area (i.e., specific sediment yield). The overall variance between the
321 two ranking techniques is shown in Figure 11a. Sub-catchments ranked 18, 21, 29, 37, 40, and
322 47 based on annual sediment yield showed substantial disagreement with the ranks assigned
323 using annual specific sediment yield (Figure 11b).

3.5 Examining the authenticity of the SSI with physically-based modelling

Sediment fingerprinting and the INVEST-SDR model were used to generate independent predictions. Here, the sediment fingerprinting based SSI technique generated estimates of relative source contributions for surface sediments collected in the reservoir, while the INVEST-SDR model generated sediment yield estimates for the four land use groups. Using results from INVEST-SDR as an independent evaluation, we computed the overall accuracy of the SSI ranking method by employing a confusion matrix for the sediment yield (Figure 12). Agreement between the annual specific sediment yield and the SSI approach was better than that with the annual sediment yield of the sub-catchments with all the prior based models. The P0 and P2 based models (i.e., no prior and silt-based priors) exhibited the lowest level of accuracy over both time frames, whereas models based on P1 and P4 (i.e., clay and slope priors, respectively) displayed the highest levels of accuracy (80% and 68% with t/ha/year and t/year, respectively) (Figure 12). The P3 (very fine sand-based prior) model predictions of the sub-catchment sediment output was ~65% accurate. Over the two time frames, the clay and slope-based priors performed the best.

4. Discussion

4.1 Multiple prior based geochemical sediment source fingerprinting

The DFA findings on the geochemical tracers showed some overlap between the source groups. Several other investigations have reported similar issues using geochemical data.

The PSD of target sediment can be affected by several factors, including the PSD of the sources, erosion patterns and intensity, and catchment slopes. It is therefore important to consider particle size carefully when using the sediment fingerprinting approach (Lacey et al., 2017; Koiter et al., 2018). Accordingly, particle size based priors were used with slope when applying the MixSIAR model. The Bayesian model with no priors (P0) identified agricultural lands as the most important sediment source (i.e. contributing ~40-55%), with human

1 349 settlement contributing 8-15%, whereas the barren lands contributed 20 to 25%, and forest ~18
2 350 to 25%. The highest human settlement contribution was estimated using the P0 model.
3
4 351 However, the P0 model underestimated the contribution of barren lands drastically, and this
5
6
7 352 land use has been reported to be a major sediment source by other studies conducted in this
8
9
10 353 region (Das et al., 2022; Rajbanshi & Bhattacharya, 2020, 2022). The clay prior (P1) based
11
12 354 model identified barren lands as the major sediment source (~20 to 70%) followed by
13
14 355 agricultural lands (~10 to 70%) during both timeframes. Similar source estimates were
15
16
17 356 generated using the slope based prior (P4) model. This suggests that the steepness of slope in
18
19 357 the barren land areas is a major factor controlling sediment sources in the study catchment
20
21
22 358 (Mishra et al., 2022). The silt based prior model (P2) predicted similar source contributions to
23
24 359 the P0 model by identifying agricultural lands and human settlement areas as major sediment
25
26
27 360 sources. The effects of silt concentration on geochemical properties were found to be negligible
28
29 361 by Kraushaar et al., (2015) and this explains the lack of any significant difference between the
30
31
32 362 source estimates using the silt based prior and no prior (P0) models. The proportion of very
33
34 363 fine sand is highest in the bare lands; however, the prior based model for this particle size
35
36 364 fraction (P3), identified forests as the major sediment source (~20 to 50 %). A substantial
37
38
39 365 contribution of forests to sediment yield has been reported by a few previous studies
40
41 366 (Upadhayay et al., 2020).

44 367 ***4.2 Validation of sediment source fingerprinting with INVEST-SDR***

45
46
47 368 The INVEST-SDR outputs were used as an independent evaluation of the sediment
48
49 369 fingerprinting estimates. Previous studies have evaluated source fingerprinting using
50
51
52 370 physically-based modelling. A study by Palazón et al., (2016), for example, reported good
53
54 371 consistency between sediment fingerprinting results and SWAT modelling. The accuracy of the
55
56
57 372 five prior based Bayesian model in prioritizing the sub-catchments indicates that the annual
58
59 373 sediment yields for the sub-catchments agree less with the SSI results compared to annual
60
61
62
63
64
65

1 374 specific sediment yield. Similar, apportionment patterns were established in a study conducted
2
3 375 by Hamel et al., (2015) which prioritized the sub-catchments based on soil erosion alone, rather
4
5 376 than erosion and sediment delivery. The clay and slope priors based models performed better
6
7 377 than the other models with an overall accuracy of >78% (Figure 12). Previous studies on soil
8
9
10 378 erosion have illustrated how catchment slope affects erosion patterns and the PSD of mobilised
11
12 379 sediment particles (Lu et al., 2016; Vigiak et al., 2012; Wang & Shi, 2015). Further, some
13
14 380 studies have reported how variable rainfall intensity and slope conditions have resulted in
15
16
17 381 greater detachment of clay particles at the experimental scale (Kiani-Harchegani et al., 2018,
18
19 382 2019; Sadeghi et al., 2017; Zhang et al., 2018).

21 ***4.3 Limitations and future outlook***

22 383
23
24 384 There are a few limitations that must be borne in mind while interpreting the results of this
25
26 385 study. Our ability to sample the reservoir for target sediment beyond two water years was
27
28
29 386 limited by time, money, and accessibility issues, and continuous monitoring was restricted in
30
31 387 2020-2021 due to COVID19 lockdowns. Even though, the results of the prior based sediment
32
33
34 388 fingerprinting study performed well when compared to physical modelling, additional source
35
36 389 sampling campaigns (annual or seasonal) may have shown greater temporal variation in
37
38
39 390 catchment sediment source contributions. Since a single target sediment sampling location was
40
41 391 deployed, the source fingerprinting estimates must be viewed as scale-dependent and
42
43
44 392 longitudinal sampling along the stream network could be used to provide further insight into
45
46 393 the sediment dynamics of the study catchment (Koiter et al., 2013). The target sediment
47
48
49 394 samples were not age dated (Fatahi et al., 2022) and may therefore reflect sediment sources
50
51 395 over recent times rather than the present day alone. Despite the aforementioned limitations,
52
53 396 however, this novel research suggested that the prior based sediment fingerprinting procedure
54
55
56 397 provides valuable information for understanding the spatial and temporal dynamics of fine
57
58 398 sediment sources and delivery in the study catchment. Our study illustrates the benefits of
59
60
61
62
63
64
65

399 combining sediment source fingerprinting with independent approaches such as physically-
400 based modelling.

401 **5 Conclusion**

402 . The major findings of this study are as follows:

- 403 a) The geochemical fingerprints of the sources successfully discriminated between the
404 surface soil samples collected from the land use classes of the Konar study catchment.
405 The sensitivity of the Bayesian model predictions to priors based on particle size and
406 slope was evaluated. The model comparisons suggested that agricultural and barren
407 lands are the most important sediment sources.
- 408 b) The performance of INVEST-SDR was satisfactory using the observed datasets from
409 the Nagwan gauging station ($R^2=0.81$ and $RMSE = 6.85$ tons/ha/Year). The two sub-
410 catchment ranking scenarios using the outputs from INVEST-SDR showed
411 disagreements in terms of the higher ranking sub-catchments. However, there were
412 some similarities between the prioritization based on both ranking schemes.
- 413 c) Comparison between the two INVEST-SDR ranking schemes and the results of the SSI
414 technique based on five prior based Bayesian models for prioritising the sub-
415 catchments was informative. The overall accuracy of the SSI method considering all
416 the models with the first ranking scheme (i.e., annual sediment yield) varied from 25-
417 62%, whereas, based on the second scheme (i.e., annual specific sediment yield) it
418 ranged between 68-82%. The performance of slope and clay prior based models
419 performed best with > 78% accuracy.

420
421
422
423
424
425
426
427

428
1 429
2 430
3 431
4 432
5 433
6 433
7 434
8 435
9 436
10 437
11 438
12 439
13 440
14 441
15 442
16 443
17 444
18 445
19 446
20 447
21 448
22 449
23 450
24 451
25 452
26 453
27 454
28 455
29 456
30 457
31 458
32
33
34
35
36
37
38
39
40
41
42
43
44
45
46
47
48
49
50
51
52
53
54
55
56
57
58
59
60
61
62
63
64
65

References

Abban, B., (Thanos) Papanicolaou, A. N., Cowles, M. K., Wilson, C. G., Abaci, O., Wacha, K., Schilling, K., & Schnoebelen, D. (2016). An enhanced Bayesian fingerprinting framework for studying sediment source dynamics in intensively managed landscapes. *Water Resources Research*, 52(6), 4646–4673.
<https://doi.org/10.1002/2015WR018030>

Afshar, S., Shamsai, A., & Saghafian, B. (2016). Dam sediment tracking using spectrometry and Landsat 8 satellite image, Taleghan Basin, Iran. *Environmental Monitoring and Assessment*, 188(2), 104. <https://doi.org/10.1007/s10661-015-5052-y>

Aneseyee, A. B., Elias, E., Soromessa, T., & Feyisa, G. L. (2020). Land use/land cover change effect on soil erosion and sediment delivery in the Winike watershed, Omo Gibe Basin, Ethiopia. *Science of The Total Environment*, 728, 138776.
<https://doi.org/10.1016/j.scitotenv.2020.138776>

Billheimer, D. (2001). Compositional receptor modeling. *Environmetrics*, 12(5), 451–467.
<https://doi.org/10.1002/env.472>

Boardman, J. (2016). The value of Google Earth™ for erosion mapping. *CATENA*, 143, 123–127. <https://doi.org/10.1016/j.catena.2016.03.031>

- 1
2
3
4
5
6
7
8
9
10
11
12
13
14
15
16
17
18
19
20
21
22
23
24
25
26
27
28
29
30
31
32
33
34
35
36
37
38
39
40
41
42
43
44
45
46
47
48
49
50
51
52
53
54
55
56
57
58
59
60
61
62
63
64
65
- 459 Borselli, L., Cassi, P., & Torri, D. (2008). Prolegomena to sediment and flow connectivity in
460 the landscape: A GIS and field numerical assessment. *CATENA*, 75(3), 268–277.
461 <https://doi.org/10.1016/j.catena.2008.07.006>
- 462 Boudreault, M., Koiter, A. J., Lobb, D. A., Liu, K., Benoy, G., Owens, P. N., & Li, S. (2019).
463 Comparison of sampling designs for sediment source fingerprinting in an agricultural
464 watershed in Atlantic Canada. *Journal of Soils and Sediments*, 19(9), 3302–3318.
465 <https://doi.org/10.1007/s11368-019-02306-6>
- 466 Carter, J., Owens, P., Walling, D., & Leeks, G. (2003). Fingerprinting suspended sediment
467 sources in a large urban river system. *The Science of The Total Environment*, 314–
468 316, 513–534. [https://doi.org/10.1016/S0048-9697\(03\)00071-8](https://doi.org/10.1016/S0048-9697(03)00071-8)
- 469 Collins, A. L. (2020). Sediment source fingerprinting: Benchmarking recent outputs,
470 remaining challenges and emerging themes. *J Soils Sediments*, [https://doi.org/](https://doi.org/10.1007/s11368-020-02755-4)
471 [10.1007/s11368-020-02755-4](https://doi.org/10.1007/s11368-020-02755-4).
- 472 Collins, A. L., Blackwell, M., Boeckx, P., Chivers, C.-A., Emelko, M., Evrard, O., Foster, I.,
473 Gellis, A., Gholami, H., Granger, S., Harris, P., Horowitz, A. J., Laceby, J. P.,
474 Martinez-Carreras, N., Minella, J., Mol, L., Nosrati, K., Pulley, S., Silins, U., ...
475 Zhang, Y. (2020). Sediment source fingerprinting: Benchmarking recent outputs,
476 remaining challenges and emerging themes. *Journal of Soils and Sediments*, 20(12),
477 4160–4193. <https://doi.org/10.1007/s11368-020-02755-4>
- 478 Collins, A. L., Pulley, S., Foster, I. D. L., Gellis, A., Porto, P., & Horowitz, A. J. (2017).
479 Sediment source fingerprinting as an aid to catchment management: A review of the
480 current state of knowledge and a methodological decision-tree for end-users. *Journal*
481 *of Environmental Management*, 194, 86–108.
482 <https://doi.org/10.1016/j.jenvman.2016.09.075>

- 483 Collins, A. L., & Walling, D. E. (2002). Selecting fingerprint properties for discriminating
1
2 484 potential suspended sediment sources in river basins. *Journal of Hydrology*,
3
4
5 485 [https://doi.org/10.1016/S0022-1694\(02\)00011-2](https://doi.org/10.1016/S0022-1694(02)00011-2).
6
- 7 486 Collins, A. L., & Walling, D. E. (2007). The storage and provenance of fine sediment on the
8
9
10 487 channel bed of two contrasting lowland permeable catchments, UK. *River Research
11
12 488 and Applications*, 23(4), 429–450. <https://doi.org/10.1002/rra.992>
13
- 14 489 Collins, A. L., & Walling, D. E. (2016). Documenting catchment suspended sediment
15
16 490 sources: Problems, approaches and prospects. *Progress in Physical Geography: Earth
17
18
19 491 and Environment*, 28(2), 159–196. <https://doi.org/10.1191/0309133304pp409ra>
20
21
- 22 492 Collins, A. L., Walling, D. E., & Leeks, G. J. I. (1997). Fingerprinting the origin of fluvial
23
24 493 suspended sediment in larger river basins: Combining assessment of spatial
25
26 494 provenance and source type. *Geografiska Annaler: Series A, Physical Geography*,
27
28 495 79(4), 239–254. <https://doi.org/10.1111/j.0435-3676.1997.00020.x>
29
30
- 31 496 Das, A., Remesan, R., Chakraborty, S., & Kumar Gupta, A. (2022). Investigation of human-
32
33 497 induced land use dynamics in a representative catchment on the Chota Nagpur
34
35 498 Plateau, India: A spatiotemporal application of soil erosion modeling with
36
37 499 connectivity index studies. *CATENA*, 217, 106524.
38
39
40
41 500 <https://doi.org/10.1016/j.catena.2022.106524>
42
- 43 501 Davis, C. M., & Fox, J. F. (2009). Sediment Fingerprinting: Review of the Method and
44
45 502 Future Improvements for Allocating Nonpoint Source Pollution. *Journal of
46
47 503 Environmental Engineering*, 135(7), 490–504. [https://doi.org/10.1061/\(ASCE\)0733-
50
51 505 9372\(2009\)135:7\(490\)
52](https://doi.org/10.1061/(ASCE)0733-
48
49 504 9372(2009)135:7(490)
- 53 505 DEMIGUEL, E., CHARLESWORTH, S., ORDONEZ, A., & SEIJAS, E. (2005).
54
55 506 Geochemical fingerprints and controls in the sediments of an urban river: River
56
57
58
59
60
61
62
63
64
65

507 Manzanares, Madrid (Spain). *Science of The Total Environment*, 340(1–3), 137–148.

508 <https://doi.org/10.1016/j.scitotenv.2004.07.031>

509 D’Haen, K., Duser, B., Verstraeten, G., Degryse, P., & De Brue, H. (2013). A sediment

510 fingerprinting approach to understand the geomorphic coupling in an eastern

511 Mediterranean mountainous river catchment. *Geomorphology*, 197, 64–75.

512 <https://doi.org/10.1016/j.geomorph.2013.04.038>

513 Fatahi, A., Gholami, H., Esmaeilpour, Y., & Fathabadi, A. (2022). Fingerprinting the spatial

514 sources of fine-grained sediment deposited in the bed of the Mehran River, southern

515 Iran. *Scientific Reports*, 12(1), 3880. <https://doi.org/10.1038/s41598-022-07882-1>

516 Guerrero, A. I., & Rogers, T. L. (2020). Evaluating the performance of the Bayesian mixing

517 tool MixSIAR with fatty acid data for quantitative estimation of diet. *Scientific*

518 *Reports*, 10(1), 20780. <https://doi.org/10.1038/s41598-020-77396-1>

519 Hamel, P., Chaplin-Kramer, R., Sim, S., & Mueller, C. (2015). A new approach to modeling

520 the sediment retention service (InVEST 3.0): Case study of the Cape Fear catchment,

521 North Carolina, USA. *Science of The Total Environment*, 524–525, 166–177.

522 <https://doi.org/10.1016/j.scitotenv.2015.04.027>

523 Hamel, P., Falinski, K., Sharp, R., Auerbach, D. A., Sánchez-Canales, M., & Denny-Frank,

524 P. J. (2017). Sediment delivery modeling in practice: Comparing the effects of

525 watershed characteristics and data resolution across hydroclimatic regions. *Science of*

526 *The Total Environment*, 580, 1381–1388.

527 <https://doi.org/10.1016/j.scitotenv.2016.12.103>

528 Hirave, P., Nelson, D. B., Glendell, M., & Alewell, C. (2023). Land-use-based freshwater

529 sediment source fingerprinting using hydrogen isotope compositions of long-chain

530 fatty acids. *Science of The Total Environment*, 875, 162638.

531 <https://doi.org/10.1016/j.scitotenv.2023.162638>

- 532 Kiani-Harchegani, M., Sadeghi, S. H., & Asadi, H. (2018). Comparing grain size distribution
1
2 533 of sediment and original soil under raindrop detachment and raindrop-induced and
3
4 534 flow transport mechanism. *Hydrological Sciences Journal*, 63(2), 312–323.
5
6
7 535 <https://doi.org/10.1080/02626667.2017.1414218>
8
9
10 536 Kiani-Harchegani, M., Sadeghi, S. H., Singh, V. P., Asadi, H., & Abedi, M. (2019). Effect of
11
12 537 rainfall intensity and slope on sediment particle size distribution during erosion using
13
14 538 partial eta squared. *CATENA*, 176, 65–72.
15
16
17 539 <https://doi.org/10.1016/j.catena.2019.01.006>
18
19 540 Koiter, A. J., Owens, P. N., Petticrew, E. L., & Lobb, D. A. (2013). The behavioural
20
21 541 characteristics of sediment properties and their implications for sediment
22
23 542 fingerprinting as an approach for identifying sediment sources in river basins. *Earth-*
24
25
26 543 *Science Reviews*, 125, 24–42. <https://doi.org/10.1016/j.earscirev.2013.05.009>
27
28
29 544 Kraushaar, S., Schumann, T., Ollesch, G., Schubert, M., Vogel, H.-J., & Siebert, C. (2015).
30
31 545 Sediment fingerprinting in northern Jordan: Element-specific correction factors in a
32
33 546 carbonatic setting. *Journal of Soils and Sediments*, 15(10), 2155–2173.
34
35
36 547 <https://doi.org/10.1007/s11368-015-1179-2>
37
38
39 548 Laceby, J. P., Evrard, O., Smith, H. G., Blake, W. H., Olley, J. M., Minella, J. P. G., & Owens,
40
41 549 P. N. (2017). The challenges and opportunities of addressing particle size effects in
42
43 550 sediment source fingerprinting: A review. *Earth-Science Reviews*, 169, 85–103.
44
45
46 551 <https://doi.org/10.1016/j.earscirev.2017.04.009>
47
48
49 552 Laceby, J. P., & Olley, J. (2015). An examination of geochemical modelling approaches to
50
51 553 tracing sediment sources incorporating distribution mixing and elemental correlations:
52
53 554 AN EXAMINATION OF GEOCHEMICAL MODELLING APPROACHES.
54
55
56 555 *Hydrological Processes*, 29(6), 1669–1685. <https://doi.org/10.1002/hyp.10287>
57
58
59
60
61
62
63
64
65

- 556 Lake, N. F., Martínez-Carreras, N., Iffly, J. F., Shaw, P. J., & Collins, A. L. (2023). Use of a
1
2 557 submersible spectrophotometer probe to fingerprint spatial suspended sediment
3
4 558 sources at catchment scale. *Science of The Total Environment*, 873, 162332.
5
6
7 559 <https://doi.org/10.1016/j.scitotenv.2023.162332>
8
9
10 560 Legout, C., Leguédois, S., Le Bissonnais, Y., & Malam Issa, O. (2005). Splash distance and
11
12 561 size distributions for various soils. *Geoderma*, 124(3–4), 279–292.
13
14 562 <https://doi.org/10.1016/j.geoderma.2004.05.006>
15
16
17 563 Liu, Y., Walling, D. E., Yang, M., & Zhang, F. (2023). Sediment source fingerprinting and the
18
19 564 temporal variability of source contributions. *Journal of Environmental Management*,
20
21 565 338, 117835. <https://doi.org/10.1016/j.jenvman.2023.117835>
22
23
24 566 Lizaga, I. (2021). Legacy of historic land cover changes on sediment provenance tracked with
25
26 567 isotopic tracers in a Mediterranean agroforestry catchment. *Journal of Environmental*
27
28 568 *Management*, <https://doi.org/10.1016/j.jenvman.2021.112291>.
29
30
31 569 Lizaga, I., Latorre, B., Gaspar, L., & Navas, A. (2022). Combined use of geochemistry and
32
33 570 compound-specific stable isotopes for sediment fingerprinting and tracing. *Science of*
34
35 571 *The Total Environment*, 832, 154834. <https://doi.org/10.1016/j.scitotenv.2022.154834>
36
37
38 572 Lu, J., Zheng, F., Li, G., Bian, F., & An, J. (2016). The effects of raindrop impact and runoff
39
40 573 detachment on hillslope soil erosion and soil aggregate loss in the Mollisol region of
41
42 574 Northeast China. *Soil and Tillage Research*, 161, 79–85.
43
44 575 <https://doi.org/10.1016/j.still.2016.04.002>
45
46
47 576 Mishra, P. K., Rai, A., Abdelrahman, K., Rai, S. C., & Tiwari, A. (2022). Land Degradation,
48
49 577 Overland Flow, Soil Erosion, and Nutrient Loss in the Eastern Himalayas, India.
50
51 578 *Land*, 11(2), 179. <https://doi.org/10.3390/land11020179>
52
53
54 579 Nosrati, K., Fathi, Z., & Collins, A. L. (2019). Fingerprinting sub-basin spatial suspended
55
56 580 sediment sources by combining geochemical tracers and weathering indices.
57
58
59
60
61
62
63
64
65

581 *Environmental Science and Pollution Research*, 26(27), 28401–28414.
1
2 582 <https://doi.org/10.1007/s11356-019-06024-x>
3
4
5 583 Palazón, L., Gaspar, L., Latorre, B., Blake, W. H., & Navas, A. (2014). Evaluating the
6
7 584 importance of surface soil contributions to reservoir sediment in alpine environments:
8
9 585 A combined modelling and fingerprinting approach in the Posets-Maladeta Natural
10
11 586 Park. *Solid Earth*, 5(2), 963–978. <https://doi.org/10.5194/se-5-963-2014>
12
13
14 587 Palazón, L., Latorre, B., Gaspar, L., Blake, W. H., Smith, H. G., & Navas, A. (2016).
15
16 588 Combining catchment modelling and sediment fingerprinting to assess sediment
17
18 589 dynamics in a Spanish Pyrenean river system. *Science of The Total Environment*, 569–
19
20 590 570, 1136–1148. <https://doi.org/10.1016/j.scitotenv.2016.06.189>
21
22
23
24 591 Rajbanshi, J., & Bhattacharya, S. (2020). Assessment of soil erosion, sediment yield and
25
26 592 basin specific controlling factors using RUSLE-SDR and PLSR approach in Konar
27
28 593 river basin, India. *Journal of Hydrology*, 587, 124935.
29
30 594 <https://doi.org/10.1016/j.jhydrol.2020.124935>
31
32
33
34 595 Rajbanshi, J., & Bhattacharya, S. (2022). Modelling the impact of climate change on soil
35
36 596 erosion and sediment yield: A case study in a sub-tropical catchment, India. *Modeling*
37
38 597 *Earth Systems and Environment*, 8(1), 689–711. <https://doi.org/10.1007/s40808-021->
39
40 598 01117-4
41
42
43 599 Reza Vaezi, A., Sadeghian, N., & Cerdà, A. (2020). Particle size distribution of sediment
44
45 600 detached from rills under raindrop impact in semi-arid soils. *Journal of Hydrology*,
46
47 601 590, 125317. <https://doi.org/10.1016/j.jhydrol.2020.125317>
48
49
50
51 602 Sadeghi, S. H., Kiani Harchegani, M., & Asadi, H. (2017). Variability of particle size
52
53 603 distributions of upward/downward splashed materials in different rainfall intensities
54
55 604 and slopes. *Geoderma*, 290, 100–106. <https://doi.org/10.1016/j.geoderma.2016.12.007>
56
57
58
59
60
61
62
63
64
65

- 605 Sharma, A., Weindorf, D. C., Man, T., Aldabaa, A. A. A., & Chakraborty, S. (2014).
1
2 606 Characterizing soils via portable X-ray fluorescence spectrometer: 3. Soil reaction
3
4 607 (pH). *Geoderma*, 232–234, 141–147. <https://doi.org/10.1016/j.geoderma.2014.05.005>
5
6
7 608 Small, I. F., Rowan, J. S., & Franks, S. W. (2002). Quantitative sediment fingerprinting using
8
9 609 a Bayesian uncertainty estimation framework. *The Structure. Function and*
10
11 610 *Management Implications of Fluvial Sedimentary Systems (Proceedings of an*
12
13 611 *International Symposium Licld at Alice Springs, Australia.*, IAHS-AISH Publication
14
15 612 276: 443-450, 2002, <https://eurekamag.com/research/003/905/003905049.php>.
16
17
18
19 613 Stock, B. C., Jackson, A. L., Ward, E. J., Parnell, A. C., Phillips, D. L., & Semmens, B. X.
20
21 614 (2018). Analyzing mixing systems using a new generation of Bayesian tracer mixing
22
23 615 models. *PeerJ*, 6, e5096. <https://doi.org/10.7717/peerj.5096>
24
25
26 616 Tang, Q., Fu, B., Wen, A., Zhang, X., He, X., & Collins, A. L. (2019). Fingerprinting the
27
28 617 sources of water-mobilized sediment threatening agricultural and water resource
29
30 618 sustainability: Progress, challenges and prospects in China. *Science China Earth*
31
32 619 *Sciences*, 62(12), 2017–2030. <https://doi.org/10.1007/s11430-018-9349-0>
33
34
35
36 620 Tiecher, T., Caner, L., Minella, J. P. G., Evrard, O., Mondamert, L., Labanowski, J., &
37
38 621 Rheinheimer, D. dos S. (2017). Tracing Sediment Sources Using Mid-infrared
39
40 622 Spectroscopy in Arvorezinha Catchment, Southern Brazil: Mid-infrared Spectroscopy
41
42 623 for Tracing Sediment Sources. *Land Degradation & Development*, 28(5), 1603–1614.
43
44 624 <https://doi.org/10.1002/ldr.2690>
45
46
47
48 625 Tiecher, T., Minella, J. P. G., Evrard, O., Caner, L., Merten, G. H., Capoane, V., Didoné, E. J.,
49
50 626 & dos Santos, D. R. (2018). Fingerprinting sediment sources in a large agricultural
51
52 627 catchment under no-tillage in Southern Brazil (Conceição River). *Land Degradation*
53
54 628 *& Development*, 29(4), 939–951. <https://doi.org/10.1002/ldr.2917>
55
56
57
58
59
60
61
62
63
64
65

- 629 Upadhayay, H. R., Bodé, S., Griepentrog, M., Huygens, D., Bajracharya, R. M., Blake, W. H.,
1
2 630 Dercon, G., Mabit, L., Gibbs, M., Semmens, B. X., Stock, B. C., Cornelis, W., &
3
4 631 Boeckx, P. (2017). Methodological perspectives on the application of compound-
5
6
7 632 specific stable isotope fingerprinting for sediment source apportionment. *Journal of*
8
9 633 *Soils and Sediments*, 17(6), 1537–1553. <https://doi.org/10.1007/s11368-017-1706-4>
10
11 634 Upadhayay, H. R., Lamichhane, S., Bajracharya, R. M., Cornelis, W., Collins, A. L., &
12
13 635 Boeckx, P. (2020). Sensitivity of source apportionment predicted by a Bayesian tracer
14
15 636 mixing model to the inclusion of a sediment connectivity index as an informative
16
17 637 prior: Illustration using the Kharka catchment (Nepal). *Science of The Total*
18
19 638 *Environment*, 713, 136703. <https://doi.org/10.1016/j.scitotenv.2020.136703>
20
21 639 Upadhayay, H. R., Zhang, Y., Granger, S. J., Micale, M., & Collins, A. L. (2022). Prolonged
22
23 640 heavy rainfall and land use drive catchment sediment source dynamics: Appraisal
24
25 641 using multiple biotracers. *Water Research*, 216, 118348.
26
27 642 <https://doi.org/10.1016/j.watres.2022.118348>
28
29 643 Vigerstol, K. L., & Aukema, J. E. (2011). A comparison of tools for modeling freshwater
30
31 644 ecosystem services. *Journal of Environmental Management*, 92(10), 2403–2409.
32
33 645 <https://doi.org/10.1016/j.jenvman.2011.06.040>
34
35 646 Vigiak, O., Borselli, L., Newham, L. T. H., McInnes, J., & Roberts, A. M. (2012).
36
37 647 Comparison of conceptual landscape metrics to define hillslope-scale sediment
38
39 648 delivery ratio. *Geomorphology*, 138(1), 74–88.
40
41 649 <https://doi.org/10.1016/j.geomorph.2011.08.026>
42
43 650 Wang, L., Han, X., Ding, S., Liang, T., Zhang, Y., Xiao, J., Dong, L., & Zhang, H. (2019).
44
45 651 Combining multiple methods for provenance discrimination based on rare earth
46
47 652 element geochemistry in lake sediment. *Science of The Total Environment*, 672, 264–
48
49 653 274. <https://doi.org/10.1016/j.scitotenv.2019.03.484>
50
51
52
53
54
55
56
57
58
59
60
61
62
63
64
65

- 1
2
3
4
5
6
7
8
9
10
11
12
13
14
15
16
17
18
19
20
21
22
23
24
25
26
27
28
29
30
31
32
33
34
35
36
37
38
39
40
41
42
43
44
45
46
47
48
49
50
51
52
53
54
55
56
57
58
59
60
61
62
63
64
65
- 654 Wang, L., & Shi, Z. H. (2015). Size Selectivity of Eroded Sediment Associated with Soil
655 Texture on Steep Slopes. *Soil Science Society of America Journal*, 79(3), 917–929.
656 <https://doi.org/10.2136/sssaj2014.10.0415>
- 657 Wilk, P. (2022). Expanding the Sediment Transport Tracking Possibilities in a River Basin
658 through the Development of a Digital Platform—DNS/SWAT. *Applied Sciences*,
659 12(8), 3848. <https://doi.org/10.3390/app12083848>
- 660 Wilkinson, S. N., Hancock, G. J., Bartley, R., Hawdon, A. A., & Keen, R. J. (2013). Using
661 sediment tracing to assess processes and spatial patterns of erosion in grazed
662 rangelands, Burdekin River basin, Australia. *Agriculture, Ecosystems & Environment*,
663 180, 90–102. <https://doi.org/10.1016/j.agee.2012.02.002>
- 664 Williamson, T. N., Fitzpatrick, F. A., & Kreiling, R. M. (2023). Building a library of source
665 samples for sediment fingerprinting – Potential and proof of concept. *Journal of*
666 *Environmental Management*, 333, 117254.
667 <https://doi.org/10.1016/j.jenvman.2023.117254>
- 668 Xu, Z., Belmont, P., Brahney, J., & Gellis, A. C. (2022). Sediment source fingerprinting as an
669 aid to large-scale landscape conservation and restoration: A review for the Mississippi
670 River Basin. *Journal of Environmental Management*, 324, 116260.
671 <https://doi.org/10.1016/j.jenvman.2022.116260>
- 672 Zhang, S., Chen, D., Li, F., He, L., Yan, M., & Yan, Y. (2018). Evaluating spatial variation of
673 suspended sediment rating curves in the middle Yellow River basin, China.
674 *Hydrological Processes*, 32(11), 1616–1624. <https://doi.org/10.1002/hyp.11514>

1
2
3
4
5
6
7 **The spatio-temporal dynamics of suspended sediment sources based on a novel indexing**
8
9 **approach combining Bayesian geochemical fingerprinting with physically-based**
10
11 **modelling**

12
13
14 **Arnab Das¹, Renji Remesan^{1*}, Adrian L. Collins²,**
15
16 **Ashok Kumar Gupta³**

17 ¹School of Water Resources, Indian Institute of Technology Kharagpur, India

18 ²Net Zero and Resilient Farming, Rothamsted Research, North Wyke, Okehampton
19
20 EX202SB, UK

21 ³Department of Civil Engineering, Indian Institute of Technology Kharagpur, India
22
23
24
25
26
27
28
29
30

31 **CORRESPONDING AUTHOR:**

32 Dr. RENJI REMESAN

33 School of Water Resources

34 Indian Institute of Technology Kharagpur

35 Kharagpur - 721302, India

36 E-mail: renji.remesan@swr.iitkgp.ac.in

37
38
39 Tel: +91-3222-281888 (Off)

40
41 FAX: +91 3222 282212 (Off)
42
43
44
45
46
47
48
49
50
51
52
53
54
55
56
57
58
59
60
61
62
63
64
65

1
2
3
4
5
6
7
8
9
10
11
12
13
14
15
16
17
18
19
20
21
22
23
24
25
26
27
28
29
30
31
32
33
34
35
36
37
38
39
40
41
42
43
44
45
46
47
48
49
50
51
52
53
54
55
56
57
58
59
60
61
62
63
64
65

1 **Abstract**

2 Applications of sediment source fingerprinting continue to increase globally as the need for
3 information to support improved management of the sediment problem persists. In our novel
4 research, a Bayesian fingerprinting approach using MixSIAR was used with geochemical
5 signatures, both without and with informative priors based on particle size and slope. The
6 source estimates were compared with a newly proposed Source Sensitivity Index (SSI) and
7 outputs from the INVEST-SDR model. MixSIAR results with informative priors indicated that
8 agricultural and barren lands are the principal sediment sources (contributing ~5 to 85 % and
9 ~5 to 80% respectively during two sampling periods i.e. 2018-2019 and 2021-2022) with
10 forests being less important. The SSI spatial maps (using % clay and slope as informative
11 priors) showed > 78% agreement with the spatial map derived using the INVEST-SDR model
12 in terms of sub-catchment prioritization for spatial sediment source contributions. This study
13 demonstrates the benefits of combining geochemical sediment source fingerprinting with SSI
14 indices in larger catchments where the spatial prioritization of soil and water conservation is
15 both challenging but warranted.

16 **Keywords:** Sediment fingerprinting, MixSIAR model, prior information, particle size
17 distribution, INVEST model

1
2
3
4
5
6
7
8
9 28 **1. Introduction**

10
11 29 Water erosion is regarded as the most serious concern to global soil security, resulting in poorer
12 30 agriculture yields and pollution of freshwater resources and estuaries (Das et al., 2022). A
13 31 significant amount of research and policy attention is still directed towards reducing
14 32 reservoir siltation and water pollution caused by water erosion; most notably, excess fine-
15 33 grained (< 63 µm) sediment (Collins et al., 2020). Understanding water-induced soil erosion,
16 34 sediment delivery and export, and sediment source patterns is crucial for targeted management
17 35 of the impacts of human actions and natural processes on soil health and water resources.
18 36 Though erosion models can be used for screening likely erodible areas in a catchment, critical
19 37 information on sediment provenance can be obtained using sediment source fingerprinting
20 38 (Lizaga et al., 2022). In particular, it is useful to identify the areas with disproportionately high
21 39 erosion rates and connectivity with river channels, for developing optimal management
22 40 strategies (Abban et al., 2016).

23 41 Several investigations have determined the relative contributions of surface and
24 42 instream sources to sediment loads (Afshar et al., 2016; Boudreault et al., 2019; Carter et al.,
25 43 2003; Collins & Walling, 2002, 2007; Lake et al., 2023). Geochemical fingerprinting of
26 44 sediments is one of the most widely used approaches (Collins et al., 2020)~~(Collins et al.,~~
27 45 ~~(2020))~~. Information on the contributions of different land use groups can be particularly
28 46 informative for watershed management, and the ~~sediment geochemical~~ fingerprinting method
29 47 based on statistically robust geochemical signatures can, in some instances, be used for
30 48 obtaining such information (Demiguel et al., 2005; Laceby & Olley, 2015; Tiecher et al., 2018).
31 49 To link the signatures of the sampled target sediment to the signatures of the sources,
32 50 fingerprinting investigations typically combines the selected tracers (e.g., geochemical) with
33 51 statistical techniques for source discrimination and numerical unmixing models for source
34
35
36
37
38
39
40
41
42
43
44
45
46
47
48
49
50
51
52
53
54
55
56
57
58
59
60
61
62
63
64
65

1
2
3
4
5
6
7 52 apportionment. Various unmixing models have been proposed and used, including frequentist
8
9 53 and Bayesian approaches (Collins, 2020; Collins et al., 2017; Davis & Fox, 2009; D'Haen et
10
11 54 al., 2013). In order to determine the sources of target sediment, the Bayesian approach
12
13 55 combines the likelihood of current sediment source data (geochemistry) with prior knowledge
14
15 56 of sediment sources ~~in the study catchment~~ to form a posterior probability distribution of source
16
17 57 contributions (Small et al., 2002). The assumption that tracers are adequately characterized for
18
19 58 the potential source areas and the target sediment samples is eased when previous information
20
21 59 is used for model parameterisation (Billheimer, 2001). Here, it is regarded by some
22
23 60 investigators that Bayesian approaches are best for illustrating the uncertainty associated with
24
25 61 estimated sediment source contributions.

26 62 Complex landscapes, however, make it difficult to pinpoint the origins of fine-grained
27
28 63 sediment. As a result, new methods are required to provide additional insights into the interplay
29
30 64 between catchment structure, surface cover, and land use practices for determining sediment
31
32 65 source contributions (Tang et al., 2019; Xu et al., 2022). In support of this, Bayesian unmixing
33
34 66 model frameworks can include prior information ~~including that~~ for relevant catchment
35
36 67 characteristics (Stock et al., 2018; Upadhayay et al., 2017). In the existing literature, numerous
37
38 68 possibilities are discussed concerning the applicability of prior information in Bayesian
39
40 69 frameworks for understanding sediment dynamics at catchment scale. A study by Upadhayay
41
42 70 et al., (2020), for example, applied a sediment connectivity index as prior information to
43
44 71 identify the crucial land use classes of a study catchment. Similar attempts have also been made
45
46 72 by other studies by using other catchment information such as land cover area (Hirave et al.,
47
48 73 2023; Lizaga, 2021; Upadhayay et al., 2017, 2022). Beyond connectivity or land cover
49
50 74 associated risks for erosion and sediment delivery, the effect of particle size selectivity on
51
52 75 sediment source signals is widely recognised in many previous studies (Haddadchi et al., 2015;
53
54 76 Gaspar et al., 2022). When it comes to rain-induced erosion, raindrops, and slope controls the

1
2
3
4
5
6
7 77 detachment and delivery of soil particles (Lu et al., 2016). In particular, the particle size
8
9 78 distributions of sediment are useful background knowledge for elucidating soil erosion
10
11 79 processes (Legout et al., 2005; Cheraghi et al., 2016; Kiani-Harchegani et al., 2019), making
12
13 80 such understanding an effective form of prior information.

14
15 81 Despite the aforementioned importance of specific catchment characteristics, source
16
17 82 apportionment studies have not, to date, explored the sensitivity of the results to the
18
19 83 combination of mean slope and particle size.

20 84 While catchment managers are interested in the interplay between areas of high risk erosion
21
22 85 and sediment delivery, this interplay can be complex, especially in large river catchments, and
23
24 86 the sediment fingerprinting technique is a powerful tool to enhance the understanding of
25
26 87 sediment contributions from different types of sources in the watershed (such as land use
27
28 88 classes, geological units, and tributary sub-catchments). Though the sediment fingerprinting
29
30 89 technique is a powerful tool to enhance the understanding of sediment contributions from
31
32 90 various types of sources in the watershed (e.g., land use classes, geological units, and tributary
33
34 91 sub-catchments), catchment managers are also interested in the interplay between areas of high
35
36 92 risk erosion and sediment delivery and such interplay can be complex, especially in large river
37
38 93 catchments. Here, combining sediment fingerprinting methods with physical erosion modelling
39
40 94 and other indices has been shown to improve the efficacy of management decisions [e.g.
41
42 95 (Palazón et al., 2014, 2016; Wilkinson et al., 2013)]. By combining the application of
43
44 96 physically-based modelling and sediment fingerprinting methods at the catchment scale, it is
45
46 97 possible to create novel indicators of the spatio-temporal variability of sediment sources [i.e.
47
48 98 source sensitivity index (SSI)]. Previous studies have, for instance, shown the value of
49
50 99 combining weathering indices with conventional geochemical tracers to gain further insight
51
52 100 into sub-basin spatial suspended sediment sources (Nosrati et al., 2019)]. Integrating indices
53
54 101 with sediment fingerprinting results can help to: (i) elucidate sub-catchment scale erosion
55
56
57
58
59
60
61
62
63
64
65

1
2
3
4
5
6
7
8
9
10
11
12
13
14
15
16
17
18
19
20
21
22
23
24
25
26
27
28
29
30
31
32
33
34
35
36
37
38
39
40
41
42
43
44
45
46
47
48
49
50
51
52
53
54
55
56
57
58
59
60
61
62
63
64
65

processes spatially, (ii) improve the accuracy of sediment source fingerprinting, and; (iii) support comparisons between sediment fingerprinting results and physical modelling outputs as a weight-of-evidence approach to understanding catchment sediment dynamics. Developing SSI can address sampling uncertainties and the spatial limitations frequently associated with sediment fingerprinting results (Collins, 2020; Collins et al., 2017; Koiter et al., 2013). Previous research using the SWAT model has shown that the integration of physical modelling and tracer-based methods on large river systems greatly improves our understanding of erosion processes (Palazón et al., 2014, 2016; Wilk, 2022). Similar to the SWAT model, the INVEST-SDR model has been extensively applied to deal with a wide range of scales and issues related to sediment delivery modelling across various hydro climatic regions (Hamel et al., 2017; Vigerstol & Aukema, 2011). In order to better understand catchment-wide erosion and sediment delivery mechanisms, this study combines the RUSLE-based INVEST-SDR model with geochemical sediment source fingerprinting in the Konar catchment, India. ~~Accordingly, this study combined application of the RUSLE-based INVEST-SDR model and geochemical sediment source fingerprinting in the Konar catchment, India, to explore the scope for improving understanding of catchment-wide erosion and sediment delivery processes.~~ The specific objectives were:

- a. To apply geochemical fingerprinting to apportion suspended sediment sources in the form of land use classes.
- b. To apply a Bayesian mixing model with particle size distribution and mean slope as prior information and to examine the sensitivity of source apportionment estimates to such data.
- c. To develop an innovative index (SSI) using the geochemical fingerprinting results to generate spatio-temporal soil erosion maps.

1
2
3
4
5
6
7
8
9
10
11
12
13
14
15
16
17
18
19
20
21
22
23
24
25
26
27
28
29
30
31
32
33
34
35
36
37
38
39
40
41
42
43
44
45
46
47
48
49
50
51
52
53
54
55
56
57
58
59
60
61
62
63
64
65

d. To assess and quantify the spatial distribution of sediment sources in the study catchment using the INVEST-SDR model and compare the outputs with the sediment fingerprinting and SSI results to evaluate the accuracy of the Bayesian sediment fingerprinting method.

2 Methodology

2.1 Study area characteristics

This study was carried out in eastern India's Konar catchment (990 km²) of the Damodar River basin. The Konar catchment has diverse geo-physical terrains including high plains, moderate hills, and valleys. Elevations range between 329-882 m, with an eastern slope (Figure 1c). The climate is subtropical, with annual average rainfall of 1100-1300 mm distributed mostly (70-80%) between June and September. Summer temperatures can reach 46°C compared with lows of 4°C in the winter. The Hazaribagh district comprises more than 70 percent of the catchment area, and most of this territory is made up of forests and rocky soils. Overall, our land use categories are found in the study catchment: i.e., agricultural lands (38%), forests (36%), barren lands (14%), and human settlements (12%) (Figure 1b). Rice, groundnuts, and maize are the primary crops cultivated in the agricultural areas during the monsoon season, while wheat, mustard, and other vegetables are grown using terrace farming on uneven terrain during the off-monsoon season. Mixed deciduous and tropical dry forests predominate in the forest zones with several species of medicinal plants and timber trees including sal (*Shorea robusta*) (Forest, Environment and Climate change Department, Government of Jharkhand; <https://forest.jharkhand.gov.in>). The three most common soil types are lithosols (46%), ferric luvisols (38%), and eutric nitosols (16%) (Supplementary Figure F1).

2.2 Soil and sediment sampling

One of the main challenges of the sediment fingerprinting approach is collecting sufficient source samples for statistical reliability (Collins & Walling, 2002). To study the temporal

Field Code Changed

1
2
3
4
5
6
7 151 variation in the suspended sediment contributions from different sources, water samples were
8
9 152 collected for six time periods from the inlet of Konar reservoir (shown in Figure 1c) for two
10
11 153 alternate water years; i.e., July 2018-June 2019 and July 2021-June 2022. Three 2L swabs of
12
13 154 suspended sediment were collected at a water depth of 0-10 cm and stored in high-density
14
15 155 polyethylene bottles during these sampling periods (Wang et al., 2019). The soil sampling plan
16
17 156 was designed to cover the spatial heterogeneity of the land use classes in the study catchment
18
19 157 and Google Earth and topographic data were used to locate the sampling points (Boardman,
20
21 158 2016). Adopting a composite sampling design is a practical solution to the issue of collecting
22
23 159 enough source samples for statistical reliability when applying the sediment fingerprinting
24
25 160 approach (Collins et al., 2017; Collins & Walling, 2002; Williamson et al., 2023). To execute
26
27 161 the composite sampling approach, 105 sites distributed throughout the study catchment and
28
29 162 representative of the different land use were used. Figure 2 shows photographs taken during
30
31 163 the sampling campaign for both the land use source classes and for target sediment in the Konar
32
33 164 reservoir (details of sampling ~~protocol~~ details are shown in supplementary Table T1).
34
35 165 Composite sampling involved merging three to four sub-samples collected within a radius of
36
37 166 100 to 500 m, depending on accessibility (Collins et al., 2017). The upper ~~five~~ cm of soil
38
39 167 ~~was~~ were sampled at each source sampling location using a non-metallic trowel deployed in
40
41 168 one extensive campaign. This one-off source sampling strategy assumed that lithological
42
43 169 features remained constant through time (Tiecher et al., 2017).

44 170 *2.3 Sample preparation and laboratory analysis*

45 171 To extract suspended sediments from the bulk water samples, the samples were first
46
47 172 centrifuged, then filtered, and finally oven dried at 70 °C for 12 hours. After 12 hours of oven
48
49 173 drying, soil samples were passed through a 63 µm sieve shaker for 24 hours to avoid
50
51 174 aggregation and to extract the silt and clay fractions to improve the direct comparability of
52
53 175 source and sediment samples (Collins & Walling, 2016). Prior to the sample processing,
54
55
56
57
58
59
60
61
62
63
64
65

Formatted: Not Highlight

1
2
3
4
5
6
7 scanning of the soil and sediment samples was performed using a DP-6000 Delta Premium
8
9 portable X-ray fluorescence (PXRF) machine equipped with an Rh X-ray tube operating at 15-
10
11 40 keV. Using the instrument's Geochem Mode, the concentrations of V, Cr, Fe, Co, Ni, Cu,
12
13 Zn, W, Hg, As, Se, Pb, Bi, Rb, U, Sr, Y, Zr, Th, Mo, Ag, Cd, Sn, Sb, Ti, Mn, Mg, Al, Si, P, S,
14
15 Cl, K, and Ca were estimated (Sharma et al., 2014). The particle size characteristics of the
16
17 source and target sediment samples were measured using a Malvern Pananalytical Mastersizer
18
19 3000.

20 ***2.4 Formulation of the Bayesian framework and priors for source***

21 ***apportionment modelling***

22
23 Geochemical tracers were selected using a standard two-step process consisting of a Kruskal-
24
25 Wallis H-test for inter-group differences, and a stepwise discriminant function analysis (DFA)
26
27 for selecting a minimal set of tracers that maximises source discrimination (Collins et al.,
28
29 1997). MixSIAR, a state-of-the-art Bayesian Isotope Mixing Model (BIMM) available as a free
30
31 R package, was used to estimate sediment source apportionment (Guerrero & Rogers, 2020;
32
33 Stock et al., 2018). The geochemical tracers were entered into a concentration-dependent
34
35 MixSIAR model with and without the use of the informative priors (Upadhayay et al., 2020).
36
37 The following settings were applied for the Markov Chain Monte Carlo (MCMC) iterations:
38
39 number of chains = 3, chain length = 3,000,000, burn = 1,500,000, thin =500. Gelman-Rubin
40
41 and Geweke diagnostic statistics were used to verify model run convergence (Stock et al.,
42
43 2018). The deviance information criteria (DIC) was used to choose the best fitting model.
44
45 Means and 95% Bayesian confidence intervals (CI) were provided from posterior distributions
46
47 derived for sediment source contributions to estimate these contributions and their associated
48
49 uncertainty (Upadhayay et al., 2020). (Upadhayay et al., (2017) provide a comprehensive
50
51 description of MixSIAR, and Stock et al., (2018) provides a comprehensive mathematical
52
53 explanation of MixSIAR.
54
55
56
57
58
59
60
61
62
63
64
65

2.4.1 Prior selection

Informative priors for sediment source proportions should be selected logically with proper physical meaning (Upadhayay et al., 2020). Research suggests that rainfall-induced soil erosion occurs in primarily three phases, each of which is particle size-based (Figure 3) (Sadeghi et al., 2017; Wang & Shi, 2015). The initial stage comprises the detachment of soil particles by raindrop splash - eroding mostly very fine particles and some fine particles (Figure 3a). The second stage i.e. after a prolonged rainfall event, is characterized by an increased proportion of coarser particles and fine particles (Figure 3b). Finally, in the third stage, sediment transportation of very fine particles and lower quantities of fine and coarse particles takes place through the stream network (Figure 3c). The slope of the terrain plays a very important role in the erosion process (Reza Vaezi et al., 2020). In this study we explored the sensitivity of the source proportion estimates to the choice of particle size priors (clay <2 µm, silt 2-50 µm, and fine sand >50 µm) by adjusting the prior specification and observing the impacts on the posterior distributions generated by MixSIAR. Particle size priors were derived by determining the mean proportions of clay, silt, and very fine sand in the individual land use classes. Mean slopes of the land use groups were used to incorporate the slope priors.

2.5 Formulation of the source sensitivity index (SSI)

The sediment fingerprinting outputs provided by MixSIAR are relative and thereby do not provide information on the sediment yields from individual sources. To address this shortcoming, we developed an SSI using: (i) sediment yield factor for each land use class; (ii) proportion of area covered by each land use class in the overall catchment and the sub-catchments therein, and; (iii) information on the temporal variability of the source contribution obtained from the sediment fingerprinting analysis (Liu et al., 2023). An SSI value may be derived to show the severity of the sub-catchments by linking the area covered by the sub-

1
2
3
4
5
6
7
8
9
10
11
12
13
14
15
16
17
18
19
20
21
22
23
24
25
26
27
28
29
30
31
32
33
34
35
36
37
38
39
40
41
42
43
44
45
46
47
48
49
50
51
52
53
54
55
56
57
58
59
60
61
62
63
64
65

catchment, the land use distribution within the sub-catchment, and the temporal variations in the total catchment's sediment production. Accordingly, the SSI was estimated as:

$$S_{ef} = \frac{X_e}{A_e} \quad (e = 1:m, f = 1:n) \quad (1)$$

$$SSI_x = \left(\sum_{f=1}^n \sum_{e=1}^m \frac{S_{ef} \cdot A_{ex}}{A_x} \right) \cdot D_x \cdot P_f \quad (2)$$

- S_{ef} = sediment yield factor for land use e in the month f .
- X_e = Source contribution (land use) to the catchment sediment yield obtained from the fingerprinting approach.
- A_e = Area covered by respective land use class (e) in the catchment.
- SSI_x = Source sensitivity of sub-catchment x .
- A_{ex} = Area covered by land use class e in sub-catchment x .
- A_x = Area covered by sub-catchment x .
- D_x = Distance factor of the sub-catchment outlet (calculated as the ratio of longest flow path and distance of the sub-catchment outlet from the catchment sink where the target sediment samples were collected) (Supplementary Figure F2).
- P_f = Proportion of annual sediment yield in the respective month.

Figure 4 depicts the analytical framework used to generate spatial maps based on SSI values in our study area. This figure also shows the whole methodology of this [study paper which employings](#) physical modelling outputs to authenticate sediment fingerprinting outcomes through SSI generated spatial maps.

2.6 *RUSLE-based hydrological model development: INVEST-SDR*

Quantification and mapping of soil loss and sediment delivery in a landscape can be accomplished using the Integrated Valuation of Ecosystem Services and Tradeoffs (INVEST)- Sediment Delivery Ratio (SDR) model (Aneseyee et al., 2020). Compared to other

1
2
3
4
5
6
7
8
9
10
11
12
13
14
15
16
17
18
19
20
21
22
23
24
25
26
27
28
29
30
31
32
33
34
35
36
37
38
39
40
41
42
43
44
45
46
47
48
49
50
51
52
53
54
55
56
57
58
59
60
61
62
63
64
65

models, such as SWAT, INVEST-SDR uses less input data (Table 1) and is more flexible; it can also be modified to a given scenario and used with locally and globally accessible data and exemplifies the hydrological connectivity concept proposed by Vigiak et al., (2012). To validate the INVEST SDR model, annual simulated sediment inflow data was compared to real data collected from Damodar Valley Corporation (DVC) using root mean square error (RMSE) and the coefficient of determination (R^2).

3 Results

3.1 Catchment sediment sources using geochemical source fingerprinting

Correct and reliable use of sediment fingerprinting requires statistical analysis and interpretation of isotope tracers from sediment source end members. One of the most important step is to identify a representative set of final geochemical tracers to use in a "composite signature" to determine the origin of fine sediments. From the laboratory analysis, 24 elements were detected in the soil and sediment samples collected from the Konar catchment. To identify the set of discriminatory geochemical tracers to be used as an input to the MixSIAR, all the elements were passed through a KW test followed by DFA (Figure 5). Based on this analysis, 21 elements were selected (Fe, K, Ti, Ca, Zn, Mn, Ba, Zr, Rb, V, Cr, Sn, Ni, Sr, Pb, Cu, Ga, Sb, Ag, A, and Br). A summary of the statistical analysis for source discrimination is provided in supplementary Table T2. Furthermore, we have also shown the spatial variability of the proportional (%) presence of few elements (Fe, K, Ti and Ca) in the soil samples collected from 105 locations of the catchment (Figure 6).

3.2 Bayesian modelling results for source apportionment

MixSIAR was run with both 'no priors (P0)' and priors based on particle size and slope information for the study catchment (details of P1 to P4 are given in Table 2). During both time periods, both agricultural and barren lands were the most important sediment sources (Figure

Formatted: Highlight

1
2
3
4
5
6
7
8
9
10
11
12
13
14
15
16
17
18
19
20
21
22
23
24
25
26
27
28
29
30
31
32
33
34
35
36
37
38
39
40
41
42
43
44
45
46
47
48
49
50
51
52
53
54
55
56
57
58
59
60
61
62
63
64
65

76). The Bayesian model with no priors (P0) and with the silt based prior (P2) identified agricultural lands as the major sediment source in most of the seasons (varying from ~30-45% during the water year 2018-19 and ~30 to 60 % during the water year 2021-22) (Figure 76 a1, a2). In contrast to the other prior-based models, these two models (P0 and P2) predicted a smaller contribution of suspended sediment from agricultural areas and a larger contribution from human settlements (Figure 76 b1, b2). The clay based prior (P1) and the slope based prior (P4) model outputs, both identified barren lands as the primary source of suspended sediment (varying from ~25-75% during the water year 2018-19 and ~20 to 60 % during water year 2021-22). In contrast, the outputs of the slope based prior model suggested negligible contributions from human settlement areas compared with the other land use classes (varying between 0-5% for both water years 2018-19 and 2021-22). The very fine sand prior (P3) based model predicted a much higher contribution from forests (varying from ~20-50% during the water year 2018-19 and ~25-50% during 2021-22). Overall, all the prior based models identified agricultural land as the primary source of sediment in July 2021 (Figure 76 a2).

3.3 SSI based Bayesian modelling results for source apportionment

This study investigated the potential utility of a new index [Source Sensitivity Index (SSI)] to help the policymakers to better understand the relative impacts of sediment sources in the Konar catchment. It integrates sediment fingerprinting information with the physical controls of sediment deposition in the sub-catchments to generate an index value for ranking the sub-catchments to explain conservation urgency. To establish a link with physical modelling results, the sub-catchments were classified into five SSI classes [class1 (26-174), class2 (175-378), class3 (379-822), class4 (823-1267), class5 (1268-5266)] (Figure 87). Figure 98 displays the distribution of the sub-catchments across the SSI classes for the particle size and slope prior based model outputs, suggesting little disparity among the sub-catchments using the P0 and P2 priors based models. However, upon closer inspection, it can be seen that the number of sub-

1
2
3
4
5
6
7 299 catchments with higher SSI classes is marginally greater during 2021–2022, compared with
8
9 300 2018–2019. This SSI based information and associated maps can be used for assessing the
10
11 301 reliability of mixing model source apportionment results based on the comparison with
12
13 302 physically-based model outputs. More sub-catchments under class 5 (C5) were discovered by
14
15 303 P1 based model in both time frames, similar to the P4 based model. ~~However, While~~ it is evident
16
17 304 from the Bayesian model findings described in section 3.2 that a comparable number of sub-
18
19 305 catchments come under the prior-based models P0 and P2. Importantly, the SSI based analysis
20
21 306 demonstrated how effectively Bayesian sediment fingerprinting results can be converted into
22
23 307 translating tool to spatially explain the sediment dynamics in the Konar catchment. This SSI
24
25 308 based information and maps can be used as a criterion for assessing the reliability of mixing
26
27 309 model source apportionment results in comparison with physically based sedimentation models
28
29 310 spatial outputs.

30 ***3.4 INVEST-SDR model based results***

31 311
32 312 The assessment of sediment export using INVEST-SDR model involved computing the annual
33
34 313 soil loss, sediment connectivity, and sediment delivery ratio of the study catchment. According
35
36 314 to the coefficient of determination (R^2) and root mean square error (RMSE) values of 0.81 and
37
38 315 6.85 t/ha/year for the Nagwan gauging station, the predicted sediment export from the
39
40 316 catchment was in line with the available observed data over time (Supplementary Figure F3).
41
42 317 Using the sediment connectivity index (SCI) proposed by Borselli et al., (2008) the mean
43
44 318 sediment connectivity is estimated to be -6.326, ranging between -11.038 and 0.179 (Figure
45
46 319 [109a](#)). INVEST-SDR's estimate for soil loss ranged from 0 to 23321 t/year, with a mean soil
47
48 320 loss rate of 23.65 tonnes per year (Figure [109b](#)). The sediment delivery ratio was computed
49
50 321 based on the connectivity index and ranged from 0 to 0.322, with a corresponding mean value
51
52 322 of 0.082 (Figure [109c](#)). The spatial variation in the Konar catchment's sediment export, ranging
53
54 323 from 0 to 3490 t/year with a mean value of 11.16 t/year, is shown in Figure [109d](#). The Konar
55
56
57
58
59
60
61
62
63
64
65

1
2
3
4
5
6
7
8
9
10
11
12
13
14
15
16
17
18
19
20
21
22
23
24
25
26
27
28
29
30
31
32
33
34
35
36
37
38
39
40
41
42
43
44
45
46
47
48
49
50
51
52
53
54
55
56
57
58
59
60
61
62
63
64
65

catchment was sub-divided into 47 sub-catchments to pinpoint the crucial hot spots of soil erosion for targeting preventative measures. All sub-catchments were ranked and classified based on the sediment export in t/year (Figure 109e) and t/ha/year (Figure 109f). Here, we used two different sub-catchment ranking methods. Firstly, the sub-catchments were ranked according to their annual sediment yield, and secondly, the sub-catchments were ranked according to annual sediment yield per unit area (i.e., specific sediment yield). The overall variance between the two ranking techniques is shown in Figure 114a. Sub-catchments ranked 18, 21, 29, 37, 40, and 47 based on annual sediment yield showed substantial disagreement with the ranks assigned using annual specific sediment yield (Figure 114b).

3.5 Examining the authenticity of the SSI with physically-based modelling

Sediment fingerprinting and the INVEST-SDR model were used to generate independent predictions. Here, the sediment fingerprinting based SSI technique generated estimates of relative source contributions for surface sediments collected in the reservoir, while the INVEST-SDR model generated sediment yield estimates for the four land use groups. Using results from INVEST-SDR as an independent evaluation, we computed the overall accuracy of the SSI ranking method by employing a confusion matrix for the sediment yield (Figure 124). Agreement between the annual specific sediment yield and the SSI approach was better than that with the annual sediment yield of the sub-catchments with all the prior based models. The P0 and P2 based models (i.e., no prior and silt-based priors) exhibited the lowest level of accuracy over both time frames, whereas models based on P1 and P4 (i.e., clay and slope priors, respectively) displayed the highest levels of accuracy (80% and 68% with t/ha/year and t/year, respectively) (Figure 124). The P3 (very fine sand-based prior) model predictions of the sub-catchment sediment output was ~65% accurate. Over the two time frames, the clay and slope-based priors performed the best.

1
2
3
4
5
6
7
349 **4. Discussion**

8
9
350 ***4.1 Multiple prior based geochemical sediment source fingerprinting***

10
11
351 The DFA findings on the geochemical tracers showed some overlap between the source
12
13
352 groups. Several other investigations have reported similar issues using geochemical data.

14
15
353 The PSD of target sediment can be affected by several factors, including the PSD of the
16
17
354 sources, erosion patterns and intensity, and catchment slopes. It is therefore important to
18
19
355 consider particle size carefully when using the sediment fingerprinting approach (Lacey et al.,
20
21
356 2017; Koiter et al., 2018). Accordingly, particle size based priors were used with slope when
22
23
357 applying the MixSIAR model. The Bayesian model with no priors (P0) identified agricultural
24
25
358 lands as the most important sediment source (i.e. contributing ~40-55%), with human
26
27
359 settlement contributing 8-15%, whereas the barren lands contributed 20 to 25%, and forest ~18
28
29
360 to 25%. The highest human settlement contribution was estimated using the P0 model.

30
31
361 However, the P0 model underestimated the contribution of barren lands drastically, and this
32
33
362 land use has been reported to be a major sediment source by other studies conducted in this
34
35
363 region (Das et al., 2022; Rajbanshi & Bhattacharya, 2020, 2022). The clay prior (P1) based
36
37
364 model identified barren lands as the major sediment source (~20 to 70%) followed by
38
39
365 agricultural lands (~10 to 70%) during both timeframes. Similar source estimates were
40
41
366 generated using the slope based prior (P4) model. This suggests that the steepness of slope in
42
43
367 the barren land areas is a major factor controlling sediment sources in the study catchment
44
45
368 (Mishra et al., 2022). The silt based prior model (P2) predicted similar source contributions to
46
47
369 the P0 model by identifying agricultural lands and human settlement areas as major sediment
48
49
370 sources. The effects of silt concentration on geochemical properties were found to be negligible
50
51
371 by Kraushaar et al., (2015) and this explains the lack of any significant difference between the
52
53
372 source estimates using the silt based prior and no prior (P0) models. The proportion of very
54
55
373 fine sand is highest in the bare lands; however, the prior based model for this particle size
56
57
58
59
60
61
62
63
64
65

1
2
3
4
5
6
7
8
9
10
11
12
13
14
15
16
17
18
19
20
21
22
23
24
25
26
27
28
29
30
31
32
33
34
35
36
37
38
39
40
41
42
43
44
45
46
47
48
49
50
51
52
53
54
55
56
57
58
59
60
61
62
63
64
65

fraction (P3), identified forests as the major sediment source (~20 to 50 %). A substantial contribution of forests to sediment yield has been reported by a few previous studies (Upadhayay et al., 2020).

4.2 Validation of sediment source fingerprinting with INVEST-SDR

The INVEST-SDR outputs were used as an independent evaluation of the sediment fingerprinting estimates. Previous studies have evaluated source fingerprinting using physically-based modelling. A study by Palazón et al., (2016), for example, reported good consistency between sediment fingerprinting results and SWAT modelling. The accuracy of the five prior based Bayesian model in prioritizing the sub-catchments indicates that the annual sediment yields for the sub-catchments agree less with the SSI results compared to annual specific sediment yield. Similar, apportionment patterns were established in a study conducted by Hamel et al., (2015) which prioritized the sub-catchments based on soil erosion alone, rather than erosion and sediment delivery. The clay and slope priors based models performed better than the other models with an overall accuracy of >78% (Figure 1244). Previous studies on soil erosion have illustrated how catchment slope affects erosion patterns and the PSD of mobilised sediment particles (Lu et al., 2016; Vigiak et al., 2012; Wang & Shi, 2015). Further, some studies have reported how variable rainfall intensity and slope conditions have resulted in greater detachment of clay particles at the experimental scale (Kiani-Harchegani et al., 2018, 2019; Sadeghi et al., 2017; Zhang et al., 2018).

4.3 Limitations and future outlook

There are a few limitations that must be borne in mind ~~while~~^{when} interpreting the results of this study. Our ability to sample the reservoir for target sediment beyond two water years was limited by time, money, and accessibility issues, and continuous monitoring was restricted in 2020-2021 due to COVID19 lockdowns. Even though, the results of the prior based sediment fingerprinting study performed well when compared to physical modelling, additional source

1
2
3
4
5
6
7 399 sampling campaigns (annual or seasonal) may have shown greater temporal variation in
8
9 400 catchment sediment source contributions. Since a single target sediment sampling location was
10
11 401 deployed, the source fingerprinting estimates must be viewed as scale-dependent and
12
13 402 longitudinal sampling along the stream network could be used to provide further insight into
14
15 403 the sediment dynamics of the study catchment (Koiter et al., 2013). The target sediment
16
17 404 samples were not age dated (Fatahi et al., 2022) and may therefore reflect sediment sources
18
19 405 over recent times rather than the present day alone. Despite the ~~above~~ aforementioned
20
21 406 limitations, however, this novel research suggested that the prior based sediment fingerprinting
22
23 407 procedure provides valuable information for understanding the spatial and temporal dynamics
24
25 408 of fine sediment sources and delivery in the study catchment. Our study illustrates the benefits
26
27 409 of combining sediment source fingerprinting with independent approaches such as physically-
28
29 410 based modelling.

30 411 **5 Conclusion**

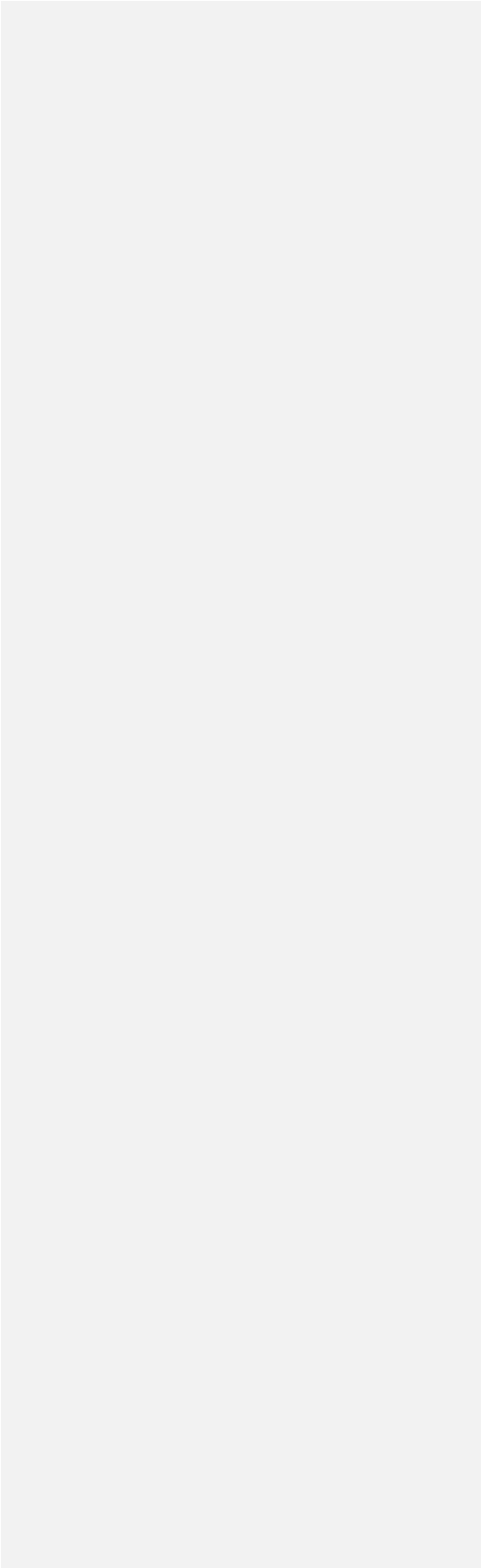
31 412 . The major findings of this study are as follows:

- 32
33 413 a) The geochemical fingerprints of the sources successfully discriminated between the
34
35 414 surface soil samples collected from the land use classes of the Konar study catchment.
36
37 415 The sensitivity of the Bayesian model predictions to priors based on particle size and
38
39 416 slope was evaluated. The model comparisons suggested that agricultural and barren
40
41 417 lands are the most important sediment sources.
- 42
43 418 b) The performance of INVEST-SDR was satisfactory using the observed datasets from
44
45 419 the Nagwan gauging station ($R^2=0.81$ and $RMSE = 6.85$ tons/haHa/Year). The two sub-
46
47 420 catchment ranking scenarios using the outputs from INVEST-SDR showed
48
49 421 disagreements in terms of the higher ranking sub-catchments. However, there were
50
51 422 some similarities between the prioritization based on both ranking schemes.

51
52
53
54
55
56
57
58
59
60
61
62
63
64
65

1
2
3
4
5
6
7
8
9
10
11
12
13
14
15
16
17
18
19
20
21
22
23
24
25
26
27
28
29
30
31
32
33
34
35
36
37
38
39
40
41
42
43
44
45
46
47
48
49
50
51
52
53
54
55
56
57
58
59
60
61
62
63
64
65

c) Comparison between the two INVEST-SDR ranking schemes and the results of the SSI technique based on five prior based Bayesian models for prioritising the sub-catchments was informative. The overall accuracy of the SSI method considering all the models with the first ranking scheme (i.e., annual sediment yield) varied from 25-62%, whereas, based on the second scheme (i.e., annual specific sediment yield) it ranged between 68-82%. The performance of slope and clay prior based models performed best with > 78% accuracy.



1
2
3
4
5
6
7
8
9
10
11
12
13
14
15
16
17
18
19
20
21
22
23
24
25
26
27
28
29
30
31
32
33
34
35
36
37
38
39
40
41
42
43
44
45
46
47
48
49
50
51
52
53
54
55
56
57
58
59
60
61
62
63
64
65

References

Abban, B., (Thanos) Papanicolaou, A. N., Cowles, M. K., Wilson, C. G., Abaci, O., Wacha, K., Schilling, K., & Schnoebelen, D. (2016). An enhanced Bayesian fingerprinting framework for studying sediment source dynamics in intensively managed landscapes. *Water Resources Research*, 52(6), 4646–4673.
<https://doi.org/10.1002/2015WR018030>

Afshar, S., Shamsai, A., & Saghafian, B. (2016). Dam sediment tracking using spectrometry and Landsat 8 satellite image, Taleghan Basin, Iran. *Environmental Monitoring and Assessment*, 188(2), 104. <https://doi.org/10.1007/s10661-015-5052-y>

Aneseyee, A. B., Elias, E., Soromessa, T., & Feyisa, G. L. (2020). Land use/land cover change effect on soil erosion and sediment delivery in the Winike watershed, Omo Gibe Basin, Ethiopia. *Science of The Total Environment*, 728, 138776.
<https://doi.org/10.1016/j.scitotenv.2020.138776>

Billheimer, D. (2001). Compositional receptor modeling. *Environmetrics*, 12(5), 451–467.
<https://doi.org/10.1002/env.472>

Boardman, J. (2016). The value of Google Earth™ for erosion mapping. *CATENA*, 143, 123–127. <https://doi.org/10.1016/j.catena.2016.03.031>

Borselli, L., Cassi, P., & Torri, D. (2008). Prolegomena to sediment and flow connectivity in the landscape: A GIS and field numerical assessment. *CATENA*, 75(3), 268–277.
<https://doi.org/10.1016/j.catena.2008.07.006>

Boudreault, M., Koiter, A. J., Lobb, D. A., Liu, K., Benoy, G., Owens, P. N., & Li, S. (2019). Comparison of sampling designs for sediment source fingerprinting in an agricultural watershed in Atlantic Canada. *Journal of Soils and Sediments*, 19(9), 3302–3318.
<https://doi.org/10.1007/s11368-019-02306-6>

- 1
2
3
4
5
6
7
490 Carter, J., Owens, P., Walling, D., & Leeks, G. (2003). Fingerprinting suspended sediment
8
9
91 sources in a large urban river system. *The Science of The Total Environment*, 314–
10
11 316, 513–534. [https://doi.org/10.1016/S0048-9697\(03\)00071-8](https://doi.org/10.1016/S0048-9697(03)00071-8)
12
13
493 Collins, A. L. (2020). Sediment source fingerprinting: Benchmarking recent outputs,
14
15 494 remaining challenges and emerging themes. *J Soils Sediments*, 34.
16
495 Collins, A. L., Blackwell, M., Boeckx, P., Chivers, C.-A., Emelko, M., Evrard, O., Foster, I.,
17
18
496 Gellis, A., Gholami, H., Granger, S., Harris, P., Horowitz, A. J., Laceby, J. P.,
19
20
497 Martinez-Carreras, N., Minella, J., Mol, L., Nosrati, K., Pulley, S., Silins, U., ...
21
22
498 Zhang, Y. (2020). Sediment source fingerprinting: Benchmarking recent outputs,
23
24 499 remaining challenges and emerging themes. *Journal of Soils and Sediments*, 20(12),
25
26 500 4160–4193. <https://doi.org/10.1007/s11368-020-02755-4>
27
501 Collins, A. L., Pulley, S., Foster, I. D. L., Gellis, A., Porto, P., & Horowitz, A. J. (2017).
28
29
502 Sediment source fingerprinting as an aid to catchment management: A review of the
30
31
503 current state of knowledge and a methodological decision-tree for end-users. *Journal*
32
33
504 *of Environmental Management*, 194, 86–108.
34
35 505 <https://doi.org/10.1016/j.jenvman.2016.09.075>
36
37 506 Collins, A. L., & Walling, D. E. (2002). Selecting fingerprint properties for discriminating
38
39 507 potential suspended sediment sources in river basins. *Journal of Hydrology*, 27.
40
508 Collins, A. L., & Walling, D. E. (2007). The storage and provenance of fine sediment on the
41
42
509 channel bed of two contrasting lowland permeable catchments, UK. *River Research*
43
44 510 *and Applications*, 23(4), 429–450. <https://doi.org/10.1002/rra.992>
45
46 511 Collins, A. L., & Walling, D. E. (2016). Documenting catchment suspended sediment
47
48 512 sources: Problems, approaches and prospects. *Progress in Physical Geography: Earth*
49
50 513 *and Environment*, 28(2), 159–196. <https://doi.org/10.1191/0309133304pp409ra>
51
52
53
54
55
56
57
58
59
60
61
62
63
64
65

1
2
3
4
5
6
7
8
9
10
11
12
13
14
15
16
17
18
19
20
21
22
23
24
25
26
27
28
29
30
31
32
33
34
35
36
37
38
39
40
41
42
43
44
45
46
47
48
49
50
51
52
53
54
55
56
57
58
59
60
61
62
63
64
65

Collins, A. L., Walling, D. E., & Leeks, G. J. I. (1997). Fingerprinting the origin of fluvial suspended sediment in larger river basins: Combining assessment of spatial provenance and source type. *Geografiska Annaler: Series A, Physical Geography*, 79(4), 239–254. <https://doi.org/10.1111/j.0435-3676.1997.00020.x>

Das, A., Remesan, R., Chakraborty, S., & Kumar Gupta, A. (2022). Investigation of human-induced land use dynamics in a representative catchment on the Chota Nagpur Plateau, India: A spatiotemporal application of soil erosion modeling with connectivity index studies. *CATENA*, 217, 106524. <https://doi.org/10.1016/j.catena.2022.106524>

Davis, C. M., & Fox, J. F. (2009). Sediment Fingerprinting: Review of the Method and Future Improvements for Allocating Nonpoint Source Pollution. *Journal of Environmental Engineering*, 135(7), 490–504. [https://doi.org/10.1061/\(ASCE\)0733-9372\(2009\)135:7\(490\)](https://doi.org/10.1061/(ASCE)0733-9372(2009)135:7(490))

DEMIGUEL, E., CHARLESWORTH, S., ORDONEZ, A., & SEIJAS, E. (2005). Geochemical fingerprints and controls in the sediments of an urban river: River Manzanares, Madrid (Spain). *Science of The Total Environment*, 340(1–3), 137–148. <https://doi.org/10.1016/j.scitotenv.2004.07.031>

D’Haen, K., Dugar, B., Verstraeten, G., Degryse, P., & De Brue, H. (2013). A sediment fingerprinting approach to understand the geomorphic coupling in an eastern Mediterranean mountainous river catchment. *Geomorphology*, 197, 64–75. <https://doi.org/10.1016/j.geomorph.2013.04.038>

Fatahi, A., Gholami, H., Esmailpour, Y., & Fathabadi, A. (2022). Fingerprinting the spatial sources of fine-grained sediment deposited in the bed of the Mehran River, southern Iran. *Scientific Reports*, 12(1), 3880. <https://doi.org/10.1038/s41598-022-07882-1>

1
2
3
4
5
6
7 538 Guerrero, A. I., & Rogers, T. L. (2020). Evaluating the performance of the Bayesian mixing
8
9 539 tool MixSIAR with fatty acid data for quantitative estimation of diet. *Scientific*
10
11 1540 *Reports*, 10(1), 20780. <https://doi.org/10.1038/s41598-020-77396-1>
12
13 541 Hamel, P., Chaplin-Kramer, R., Sim, S., & Mueller, C. (2015). A new approach to modeling
14
15 542 the sediment retention service (InVEST 3.0): Case study of the Cape Fear catchment,
16
17 543 North Carolina, USA. *Science of The Total Environment*, 524–525, 166–177.
18
19 544 <https://doi.org/10.1016/j.scitotenv.2015.04.027>
20
21 545 Hamel, P., Falinski, K., Sharp, R., Auerbach, D. A., Sánchez-Canales, M., & Dennedy-Frank,
22
23 546 P. J. (2017). Sediment delivery modeling in practice: Comparing the effects of
24
25 547 watershed characteristics and data resolution across hydroclimatic regions. *Science of*
26
27 548 *The Total Environment*, 580, 1381–1388.
28
29 549 <https://doi.org/10.1016/j.scitotenv.2016.12.103>
30
31 550 Hirave, P., Nelson, D. B., Glendell, M., & Alewell, C. (2023). Land-use-based freshwater
32
33 551 sediment source fingerprinting using hydrogen isotope compositions of long-chain
34
35 552 fatty acids. *Science of The Total Environment*, 875, 162638.
36
37 553 <https://doi.org/10.1016/j.scitotenv.2023.162638>
38
39 554 Kiani-Harchegani, M., Sadeghi, S. H., & Asadi, H. (2018). Comparing grain size distribution
40
41 555 of sediment and original soil under raindrop detachment and raindrop-induced and
42
43 556 flow transport mechanism. *Hydrological Sciences Journal*, 63(2), 312–323.
44
45 557 <https://doi.org/10.1080/02626667.2017.1414218>
46
47 558 Kiani-Harchegani, M., Sadeghi, S. H., Singh, V. P., Asadi, H., & Abedi, M. (2019). Effect of
48
49 559 rainfall intensity and slope on sediment particle size distribution during erosion using
50
51 560 partial eta squared. *CATENA*, 176, 65–72.
52
53 561 <https://doi.org/10.1016/j.catena.2019.01.006>
54
55
56
57
58
59
60
61
62
63
64
65

- 1
2
3
4
5
6
7
8
9
10
11
12
13
14
15
16
17
18
19
20
21
22
23
24
25
26
27
28
29
30
31
32
33
34
35
36
37
38
39
40
41
42
43
44
45
46
47
48
49
50
51
52
53
54
55
56
57
58
59
60
61
62
63
64
65
- 562 Koiter, A. J., Owens, P. N., Petticrew, E. L., & Lobb, D. A. (2013). The behavioural
563 characteristics of sediment properties and their implications for sediment
564 fingerprinting as an approach for identifying sediment sources in river basins. *Earth-*
565 *Science Reviews*, 125, 24–42. <https://doi.org/10.1016/j.earscirev.2013.05.009>
- 566 Kraushaar, S., Schumann, T., Ollesch, G., Schubert, M., Vogel, H.-J., & Siebert, C. (2015).
567 Sediment fingerprinting in northern Jordan: Element-specific correction factors in a
568 carbonatic setting. *Journal of Soils and Sediments*, 15(10), 2155–2173.
569 <https://doi.org/10.1007/s11368-015-1179-2>
- 570 Laceby, J. P., Evrard, O., Smith, H. G., Blake, W. H., Olley, J. M., Minella, J. P. G., & Owens,
571 P. N. (2017). The challenges and opportunities of addressing particle size effects in
572 sediment source fingerprinting: A review. *Earth-Science Reviews*, 169, 85–103.
573 <https://doi.org/10.1016/j.earscirev.2017.04.009>
- 574 Laceby, J. P., & Olley, J. (2015). An examination of geochemical modelling approaches to
575 tracing sediment sources incorporating distribution mixing and elemental correlations:
576 AN EXAMINATION OF GEOCHEMICAL MODELLING APPROACHES.
577 *Hydrological Processes*, 29(6), 1669–1685. <https://doi.org/10.1002/hyp.10287>
- 578 Lake, N. F., Martínez-Carreras, N., Iffly, J. F., Shaw, P. J., & Collins, A. L. (2023). Use of a
579 submersible spectrophotometer probe to fingerprint spatial suspended sediment
580 sources at catchment scale. *Science of The Total Environment*, 873, 162332.
581 <https://doi.org/10.1016/j.scitotenv.2023.162332>
- 582 Legout, C., Leguédou, S., Le Bissonnais, Y., & Malam Issa, O. (2005). Splash distance and
583 size distributions for various soils. *Geoderma*, 124(3–4), 279–292.
584 <https://doi.org/10.1016/j.geoderma.2004.05.006>

- 1
2
3
4
5
6
7 585 Liu, Y., Walling, D. E., Yang, M., & Zhang, F. (2023). Sediment source fingerprinting and the
8
9 586 temporal variability of source contributions. *Journal of Environmental Management*,
10
11 587 338, 117835. <https://doi.org/10.1016/j.jenvman.2023.117835>
12
13 588 Lizaga, I. (2021). Legacy of historic land cover changes on sediment provenance tracked with
14
15 589 isotopic tracers in a Mediterranean agroforestry catchment. *Journal of Environmental*
16
17 590 *Management*, 11.
18 591 Lizaga, I., Latorre, B., Gaspar, L., & Navas, A. (2022). Combined use of geochemistry and
19
20 592 compound-specific stable isotopes for sediment fingerprinting and tracing. *Science of*
21
22 593 *The Total Environment*, 832, 154834. <https://doi.org/10.1016/j.scitotenv.2022.154834>
23
24 594 Lu, J., Zheng, F., Li, G., Bian, F., & An, J. (2016). The effects of raindrop impact and runoff
25
26 595 detachment on hillslope soil erosion and soil aggregate loss in the Mollisol region of
27
28 596 Northeast China. *Soil and Tillage Research*, 161, 79–85.
29
30 597 <https://doi.org/10.1016/j.still.2016.04.002>
31
32 598 Mishra, P. K., Rai, A., Abdelrahman, K., Rai, S. C., & Tiwari, A. (2022). Land Degradation,
33
34 599 Overland Flow, Soil Erosion, and Nutrient Loss in the Eastern Himalayas, India.
35
36 600 *Land*, 11(2), 179. <https://doi.org/10.3390/land11020179>
37
38 601 Nosrati, K., Fathi, Z., & Collins, A. L. (2019). Fingerprinting sub-basin spatial suspended
39
40 602 sediment sources by combining geochemical tracers and weathering indices.
41
42 603 *Environmental Science and Pollution Research*, 26(27), 28401–28414.
43
44 604 <https://doi.org/10.1007/s11356-019-06024-x>
45
46 605 Palazón, L., Gaspar, L., Latorre, B., Blake, W. H., & Navas, A. (2014). Evaluating the
47
48 606 importance of surface soil contributions to reservoir sediment in alpine environments:
49
50 607 A combined modelling and fingerprinting approach in the Posets-Maladeta Natural
51
52 608 Park. *Solid Earth*, 5(2), 963–978. <https://doi.org/10.5194/se-5-963-2014>
53
54
55
56
57
58
59
60
61
62
63
64
65

1
2
3
4
5
6
7 609 Palazón, L., Latorre, B., Gaspar, L., Blake, W. H., Smith, H. G., & Navas, A. (2016).
8
9 610 Combining catchment modelling and sediment fingerprinting to assess sediment
10
11 611 dynamics in a Spanish Pyrenean river system. *Science of The Total Environment*, 569–
12
13 612 570, 1136–1148. <https://doi.org/10.1016/j.scitotenv.2016.06.189>
14
15 613 Rajbanshi, J., & Bhattacharya, S. (2020). Assessment of soil erosion, sediment yield and
16
17 614 basin specific controlling factors using RUSLE-SDR and PLSR approach in Konar
18
19 615 river basin, India. *Journal of Hydrology*, 587, 124935.
20
21 616 <https://doi.org/10.1016/j.jhydrol.2020.124935>
22
23 617 Rajbanshi, J., & Bhattacharya, S. (2022). Modelling the impact of climate change on soil
24
25 618 erosion and sediment yield: A case study in a sub-tropical catchment, India. *Modeling*
26
27 619 *Earth Systems and Environment*, 8(1), 689–711. [https://doi.org/10.1007/s40808-021-](https://doi.org/10.1007/s40808-021-01117-4)
28
29 620 01117-4
30
31 621 Reza Vaezi, A., Sadeghian, N., & Cerdà, A. (2020). Particle size distribution of sediment
32
33 622 detached from rills under raindrop impact in semi-arid soils. *Journal of Hydrology*,
34
35 623 590, 125317. <https://doi.org/10.1016/j.jhydrol.2020.125317>
36
37 624 Sadeghi, S. H., Kiani Harchegani, M., & Asadi, H. (2017). Variability of particle size
38
39 625 distributions of upward/downward splashed materials in different rainfall intensities
40
41 626 and slopes. *Geoderma*, 290, 100–106. <https://doi.org/10.1016/j.geoderma.2016.12.007>
42
43 627 Sharma, A., Weindorf, D. C., Man, T., Aldabaa, A. A. A., & Chakraborty, S. (2014).
44
45 628 Characterizing soils via portable X-ray fluorescence spectrometer: 3. Soil reaction
46
47 629 (pH). *Geoderma*, 232–234, 141–147. <https://doi.org/10.1016/j.geoderma.2014.05.005>
48
49 630 Small, I. F., Rowan, J. S., & Franks, S. W. (2002). Quantitative sediment fingerprinting using
50
51 631 a Bayesian uncertainty estimation framework. *The Structure. Function and*
52
53 632 *Management Implications of Fluvial Sedimentary Systems (Proceedings of an*
54
55 633 *International Symposium Liold at Alice Springs, Australia.*, 8.
56
57
58
59
60
61
62
63
64
65

1
2
3
4
5
6
7 634 Stock, B. C., Jackson, A. L., Ward, E. J., Parnell, A. C., Phillips, D. L., & Semmens, B. X.
8
9 635 (2018). Analyzing mixing systems using a new generation of Bayesian tracer mixing
10
11 636 models. *PeerJ*, 6, e5096. <https://doi.org/10.7717/peerj.5096>
12
13 637 Tang, Q., Fu, B., Wen, A., Zhang, X., He, X., & Collins, A. L. (2019). Fingerprinting the
14
15 638 sources of water-mobilized sediment threatening agricultural and water resource
16
17 639 sustainability: Progress, challenges and prospects in China. *Science China Earth
18 640 Sciences*, 62(12), 2017–2030. <https://doi.org/10.1007/s11430-018-9349-0>
19
20 641 Tiecher, T., Caner, L., Minella, J. P. G., Evrard, O., Mondamert, L., Labanowski, J., &
21
22 642 Rheinheimer, D. dos S. (2017). Tracing Sediment Sources Using Mid-infrared
23
24 643 Spectroscopy in Arvorezinha Catchment, Southern Brazil: Mid-infrared Spectroscopy
25
26 644 for Tracing Sediment Sources. *Land Degradation & Development*, 28(5), 1603–1614.
27
28 645 <https://doi.org/10.1002/ldr.2690>
29
30 646 Tiecher, T., Minella, J. P. G., Evrard, O., Caner, L., Merten, G. H., Capoane, V., Didoné, E. J.,
31
32 647 & dos Santos, D. R. (2018). Fingerprinting sediment sources in a large agricultural
33
34 648 catchment under no-tillage in Southern Brazil (Conceição River). *Land Degradation
35 649 & Development*, 29(4), 939–951. <https://doi.org/10.1002/ldr.2917>
36
37 650 Upadhayay, H. R., Bodé, S., Griepentrog, M., Huygens, D., Bajracharya, R. M., Blake, W. H.,
38
39 651 Dercon, G., Mabit, L., Gibbs, M., Semmens, B. X., Stock, B. C., Cornelis, W., &
40
41 652 Boeckx, P. (2017). Methodological perspectives on the application of compound-
42
43 653 specific stable isotope fingerprinting for sediment source apportionment. *Journal of
44 654 Soils and Sediments*, 17(6), 1537–1553. <https://doi.org/10.1007/s11368-017-1706-4>
45
46 655 Upadhayay, H. R., Lamichhane, S., Bajracharya, R. M., Cornelis, W., Collins, A. L., &
47
48 656 Boeckx, P. (2020). Sensitivity of source apportionment predicted by a Bayesian tracer
49
50 657 mixing model to the inclusion of a sediment connectivity index as an informative

51
52
53
54
55
56
57
58
59
60
61
62
63
64
65

1
2
3
4
5
6
7 prior: Illustration using the Kharka catchment (Nepal). *Science of The Total*
8
9 *Environment*, 713, 136703. <https://doi.org/10.1016/j.scitotenv.2020.136703>
10
11 Upadhayay, H. R., Zhang, Y., Granger, S. J., Micale, M., & Collins, A. L. (2022). Prolonged
12
13 heavy rainfall and land use drive catchment sediment source dynamics: Appraisal
14
15 using multiple biotracers. *Water Research*, 216, 118348.
16
17 <https://doi.org/10.1016/j.watres.2022.118348>
18
19 Vigerstol, K. L., & Aukema, J. E. (2011). A comparison of tools for modeling freshwater
20
21 ecosystem services. *Journal of Environmental Management*, 92(10), 2403–2409.
22
23 <https://doi.org/10.1016/j.jenvman.2011.06.040>
24
25 Vigiak, O., Borselli, L., Newham, L. T. H., McInnes, J., & Roberts, A. M. (2012).
26
27 Comparison of conceptual landscape metrics to define hillslope-scale sediment
28
29 delivery ratio. *Geomorphology*, 138(1), 74–88.
30
31 <https://doi.org/10.1016/j.geomorph.2011.08.026>
32
33 Wang, L., Han, X., Ding, S., Liang, T., Zhang, Y., Xiao, J., Dong, L., & Zhang, H. (2019).
34
35 Combining multiple methods for provenance discrimination based on rare earth
36
37 element geochemistry in lake sediment. *Science of The Total Environment*, 672, 264–
38
39 274. <https://doi.org/10.1016/j.scitotenv.2019.03.484>
40
41 Wang, L., & Shi, Z. H. (2015). Size Selectivity of Eroded Sediment Associated with Soil
42
43 Texture on Steep Slopes. *Soil Science Society of America Journal*, 79(3), 917–929.
44
45 <https://doi.org/10.2136/sssaj2014.10.0415>
46
47 Wilk, P. (2022). Expanding the Sediment Transport Tracking Possibilities in a River Basin
48
49 through the Development of a Digital Platform—DNS/SWAT. *Applied Sciences*,
50
51 12(8), 3848. <https://doi.org/10.3390/app12083848>
52
53 Wilkinson, S. N., Hancock, G. J., Bartley, R., Hawdon, A. A., & Keen, R. J. (2013). Using
54
55 sediment tracing to assess processes and spatial patterns of erosion in grazed
56
57
58
59
60
61
62
63
64
65

1
2
3
4
5
6
7 683 rangelands, Burdekin River basin, Australia. *Agriculture, Ecosystems & Environment*,
8 180, 90–102. <https://doi.org/10.1016/j.agee.2012.02.002>
9 684
10
11 685 Williamson, T. N., Fitzpatrick, F. A., & Kreiling, R. M. (2023). Building a library of source
12 samples for sediment fingerprinting – Potential and proof of concept. *Journal of*
13 686 *Environmental Management*, 333, 117254.
14
15 687 <https://doi.org/10.1016/j.jenvman.2023.117254>
16 688
17
18 689 Xu, Z., Belmont, P., Brahney, J., & Gellis, A. C. (2022). Sediment source fingerprinting as an
19 aid to large-scale landscape conservation and restoration: A review for the Mississippi
20 690 River Basin. *Journal of Environmental Management*, 324, 116260.
21
22 691 <https://doi.org/10.1016/j.jenvman.2022.116260>
23 692
24
25 693 Zhang, S., Chen, D., Li, F., He, L., Yan, M., & Yan, Y. (2018). Evaluating spatial variation of
26 694 suspended sediment rating curves in the middle Yellow River basin, China.
27
28 695 *Hydrological Processes*, 32(11), 1616–1624. <https://doi.org/10.1002/hyp.11514>
29
30 696
31
32 697
33 698
34 699
35
36
37
38
39
40
41
42
43
44
45
46
47
48
49
50
51
52
53
54
55
56
57
58
59
60
61
62
63
64
65

Figures

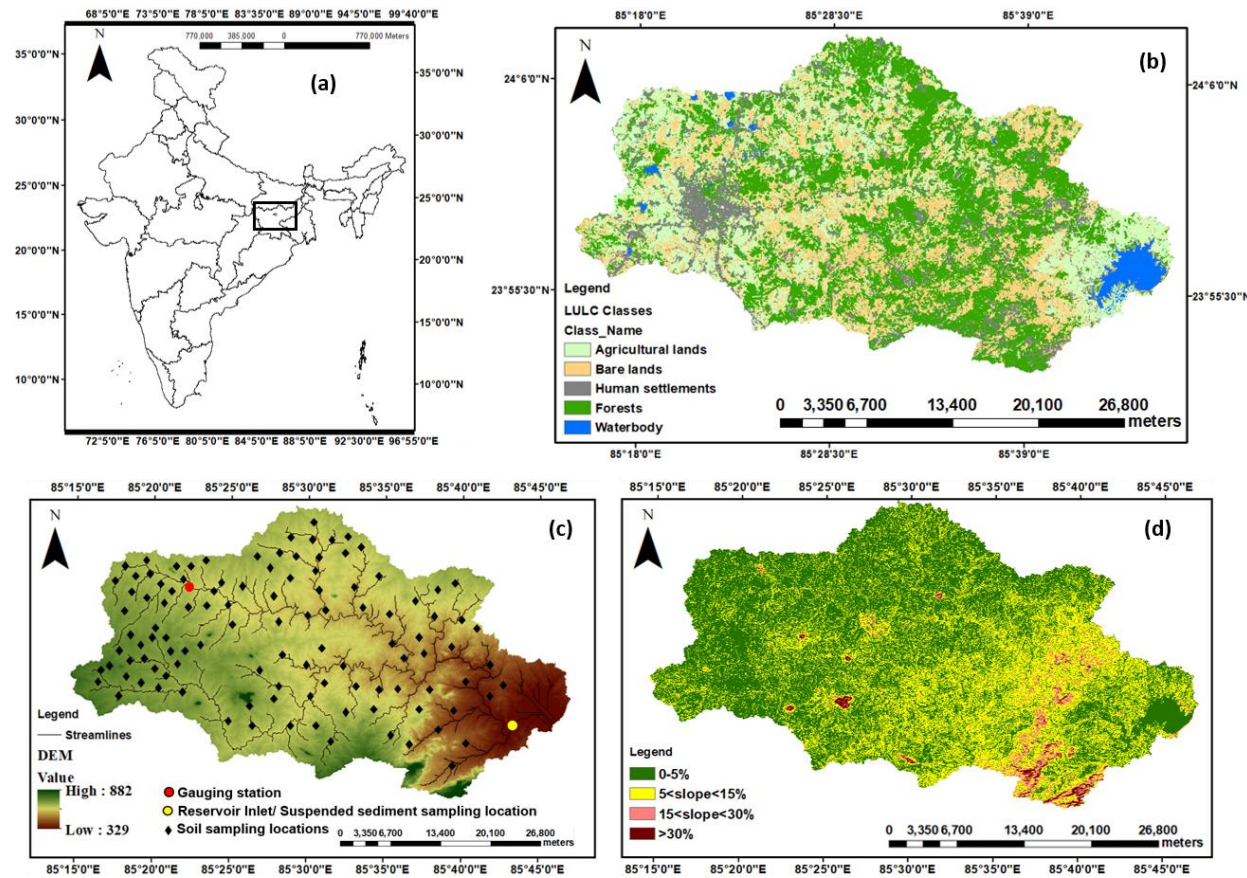


Figure 1. Information on the Konar study catchment characteristics: (a) location (b) land use (c) DEM (d) slope.

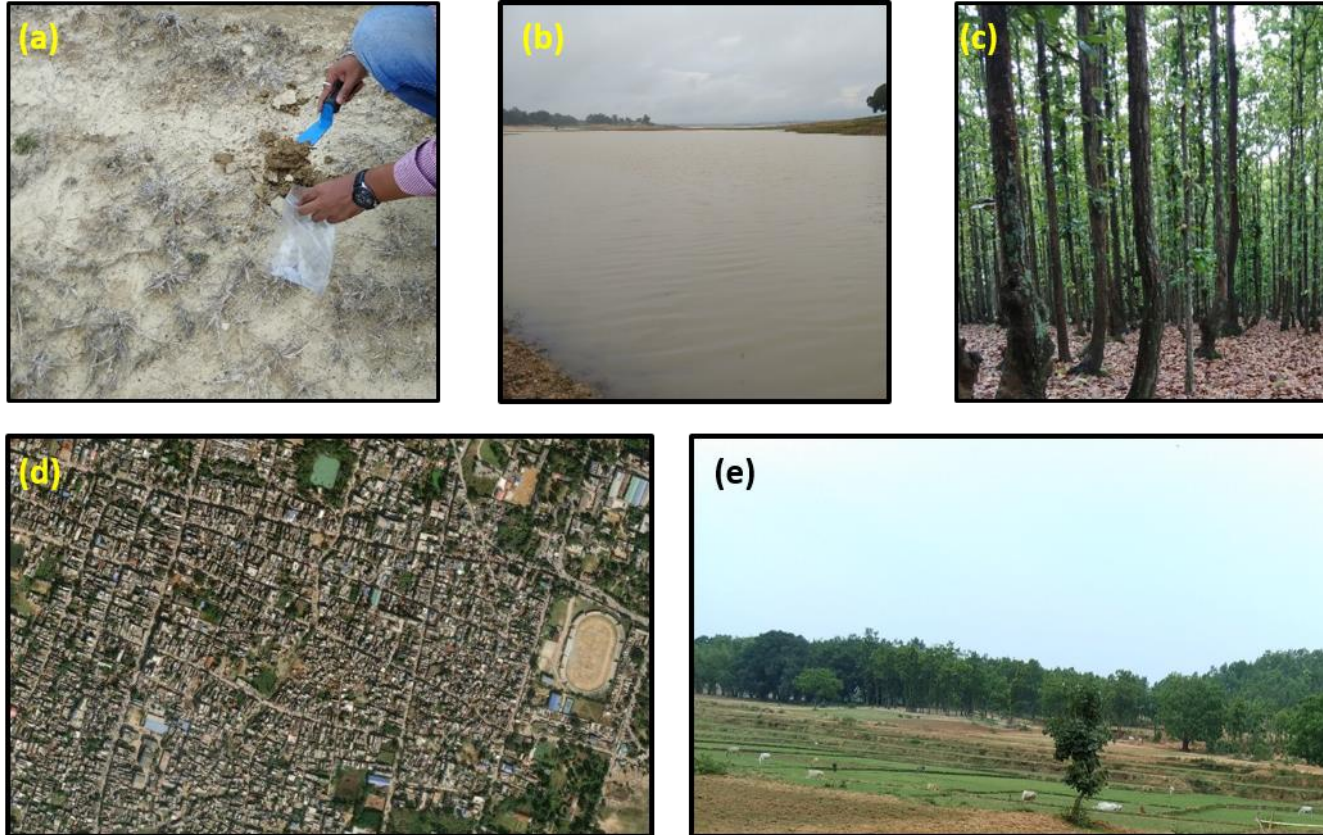


Figure 2 Land use classes of the catchment: (a) bare lands (b) Konar reservoir (c) forest (d) Human settlement (e) Agricultural fields undergoing terrace farming.

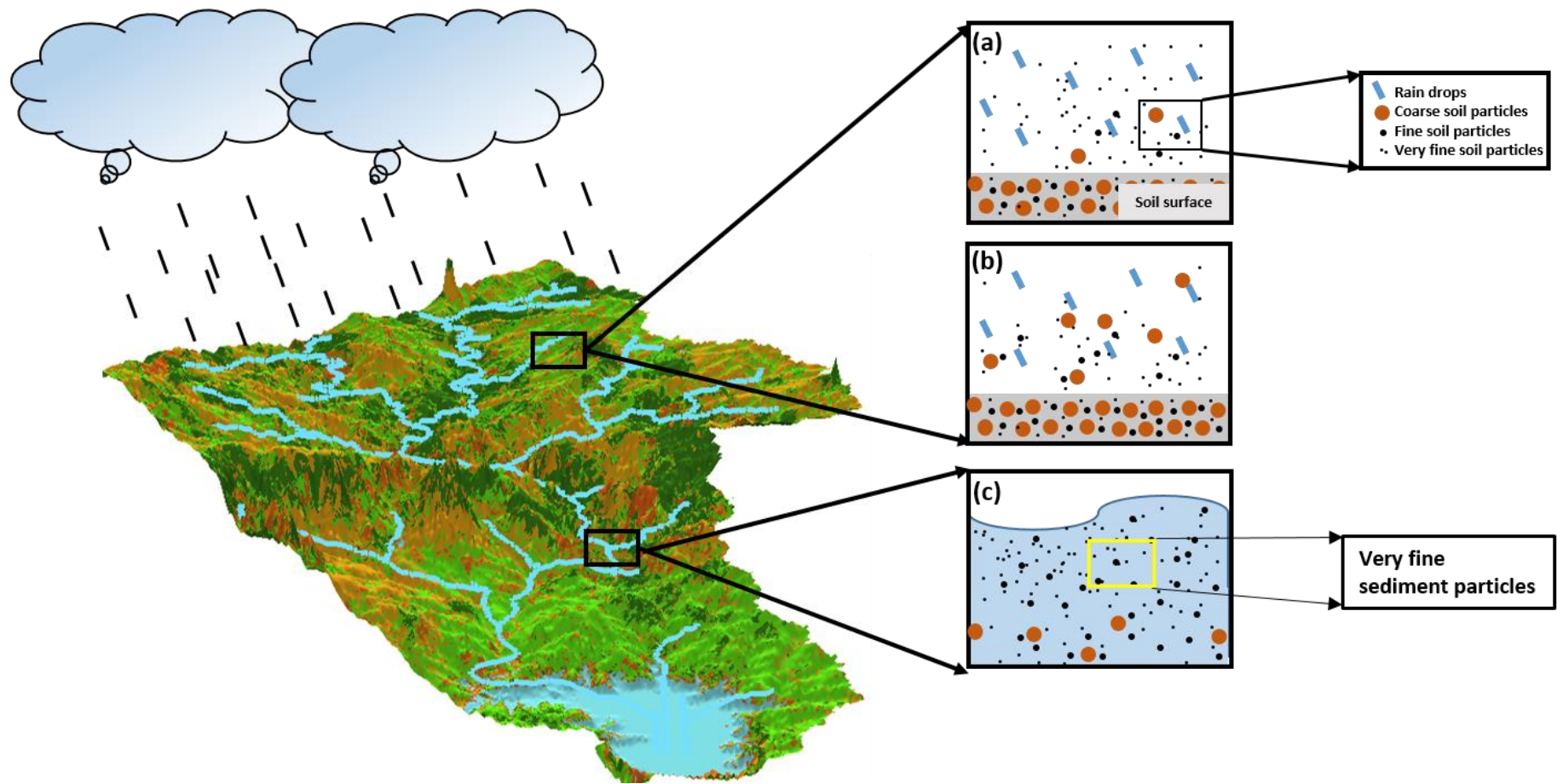


Figure 3 Conceptualisation of soil erosion scenario for prior development: (a) erosion scenario at the beginning of rainfall. (b) erosion scenario after prolonged rainfall. (c) Sediment transportation scenario.

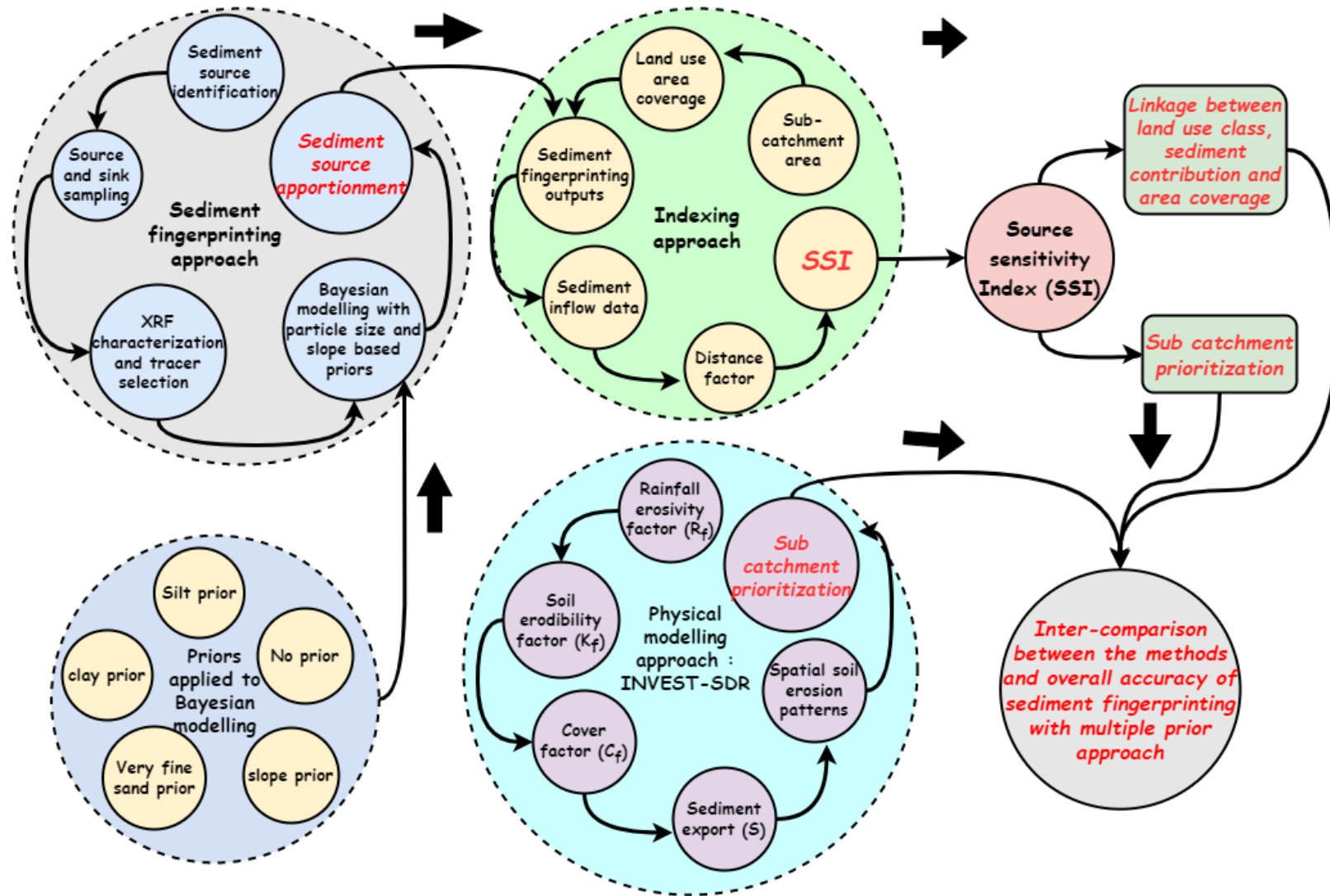


Figure 4 Methodological framework for developing the SSI.

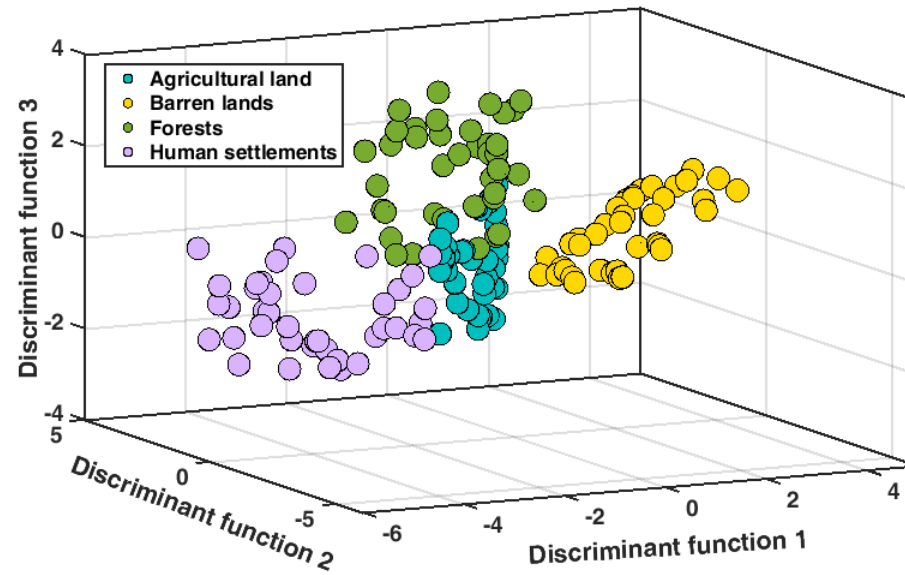


Figure 5 Results of Discriminant Function Analysis on the geochemical tracers of the source samples collected from the land use classes in the Konar study catchment.

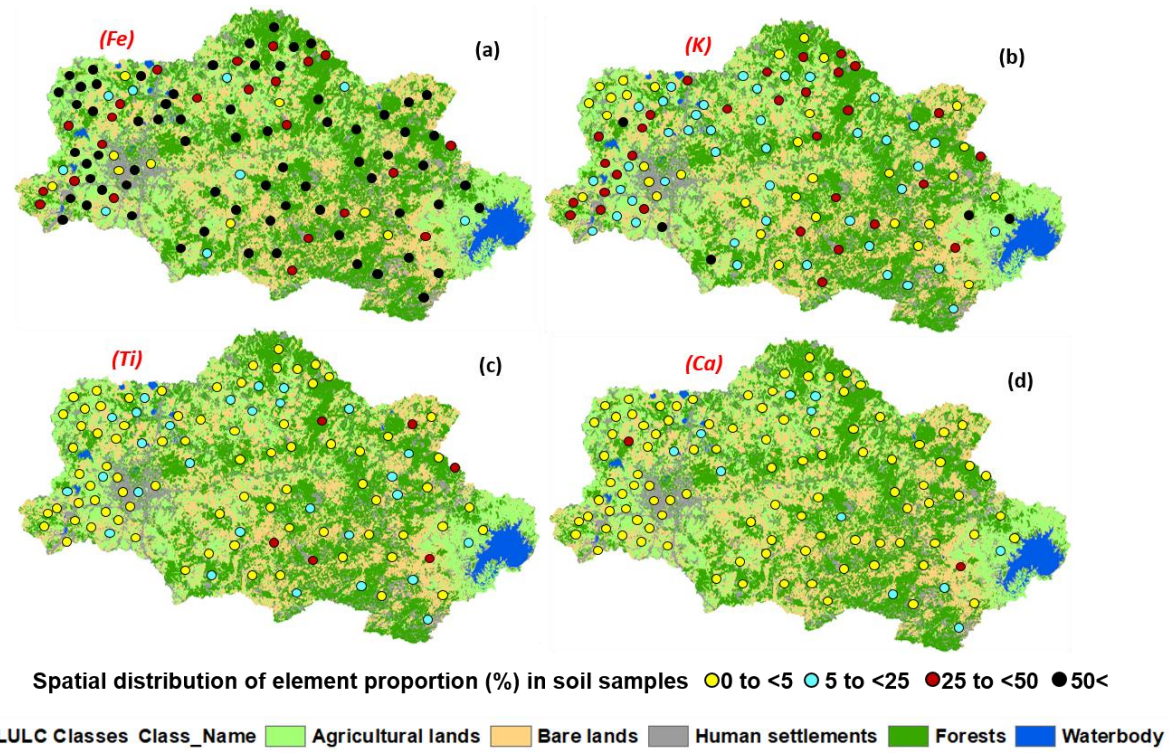


Figure 6 Spatial variation of elemental proportion (%) of (a) Fe, (b) K, (c) Ti and (d) Ca among the soil samples collected from the study catchment

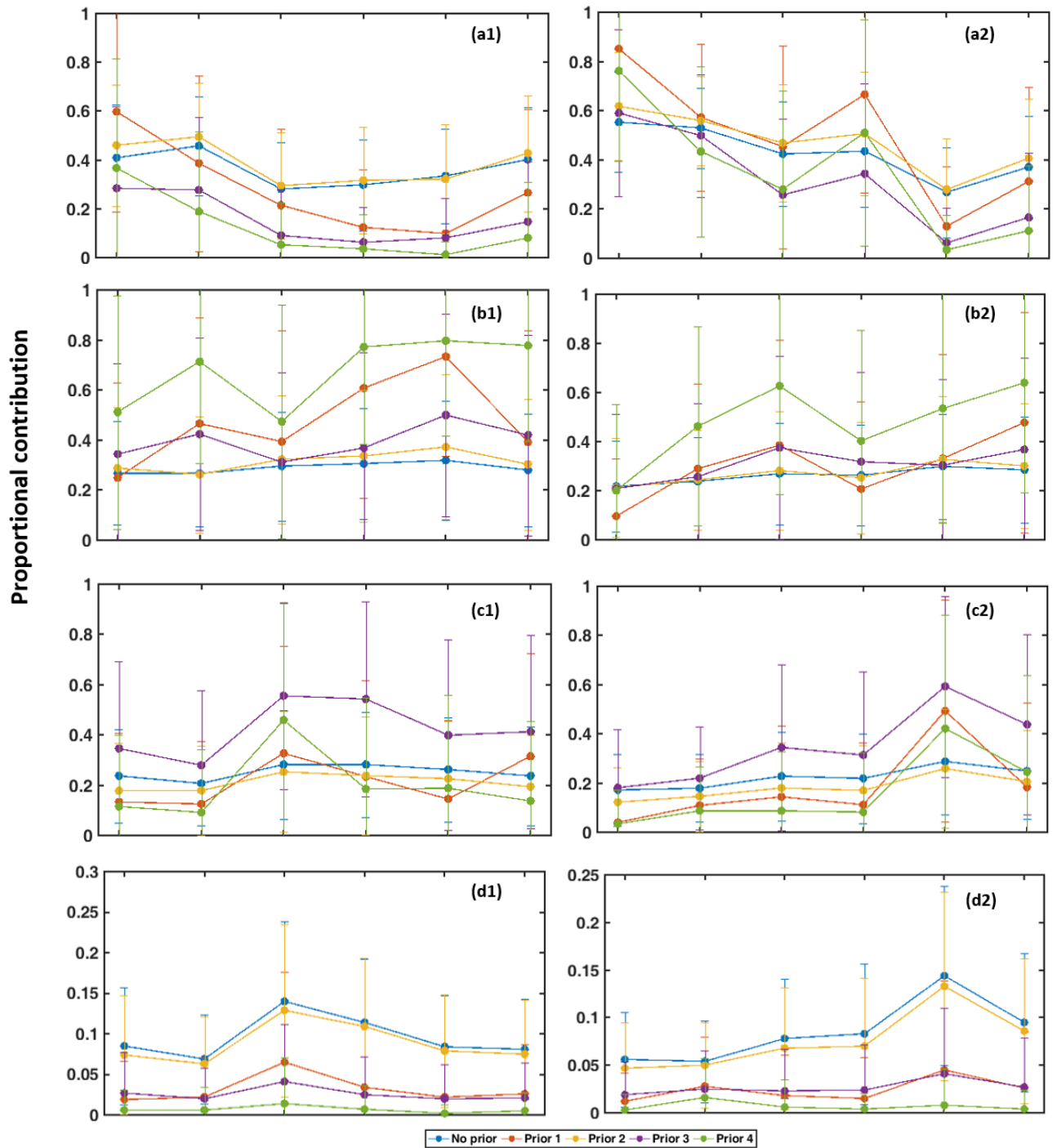


Figure 7 Temporal variation in suspended sediment source contributions (with 95% confidence intervals) using multiple priors (P0, P1, P2, P3, and P4) in MixSIAR. a1, b1, c1 and d1 represent the proportional contributions from agricultural lands, barren lands, forests and human settlements, respectively, in 2018-2019 (July, August, October, December, March and April). a2, b2, c2 and d2 represent the proportional contribution from the land use classes in 2021-2022.

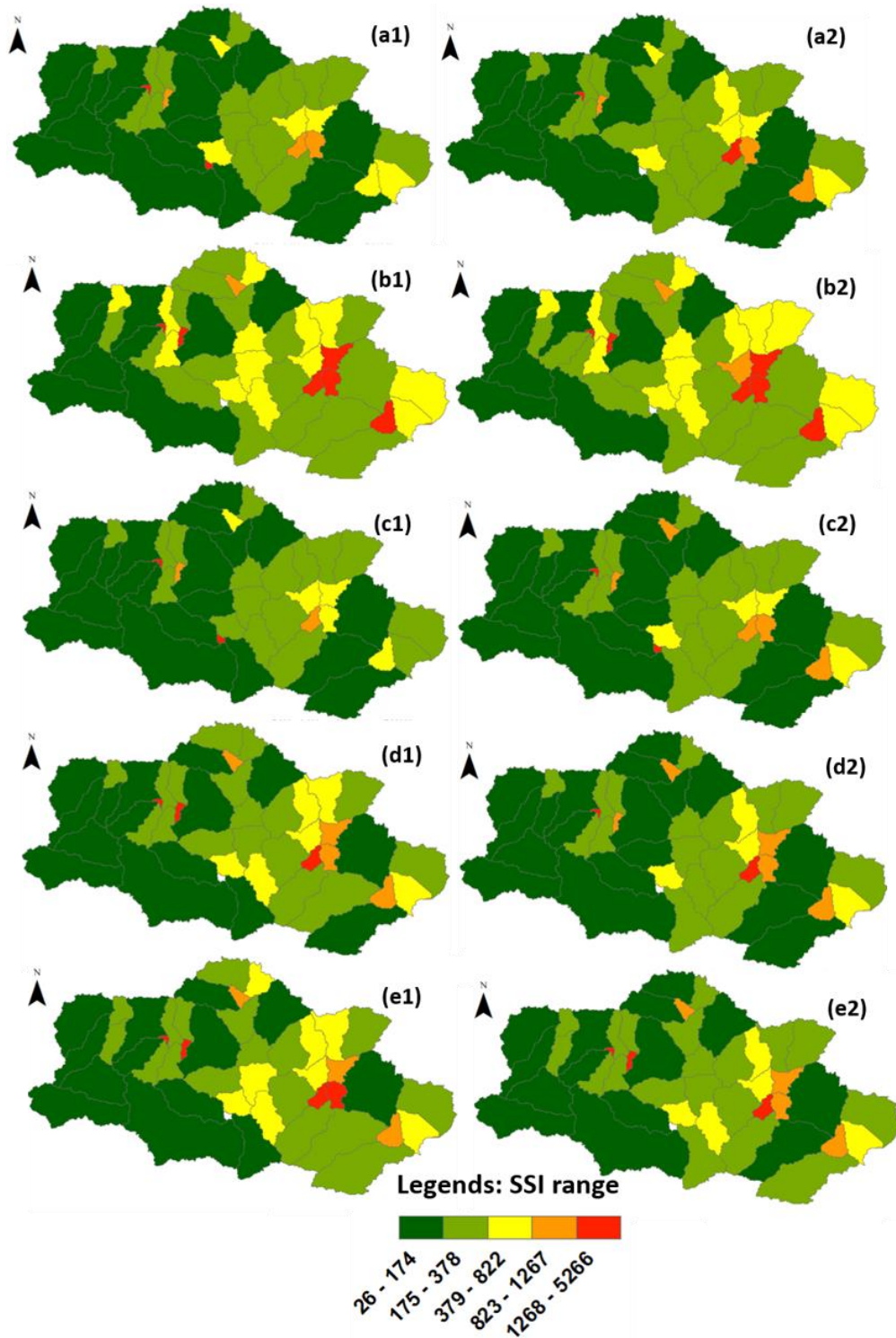


Figure 8 Spatial variation of the SSI calculated for the 47 sub-catchments in the Konar river basin. The SSI calculated using sediment fingerprinting results using multiple priors (i.e. P_0 , P_1 , P_2 , P_3 and P_4) for the period of 2018-2019 is shown in a1, b1, c1, d1, e1 and for 2021-2022 in a2, b2, c2, d2, e2.

** P_0 represents the no prior condition of the Bayesian modeling study.

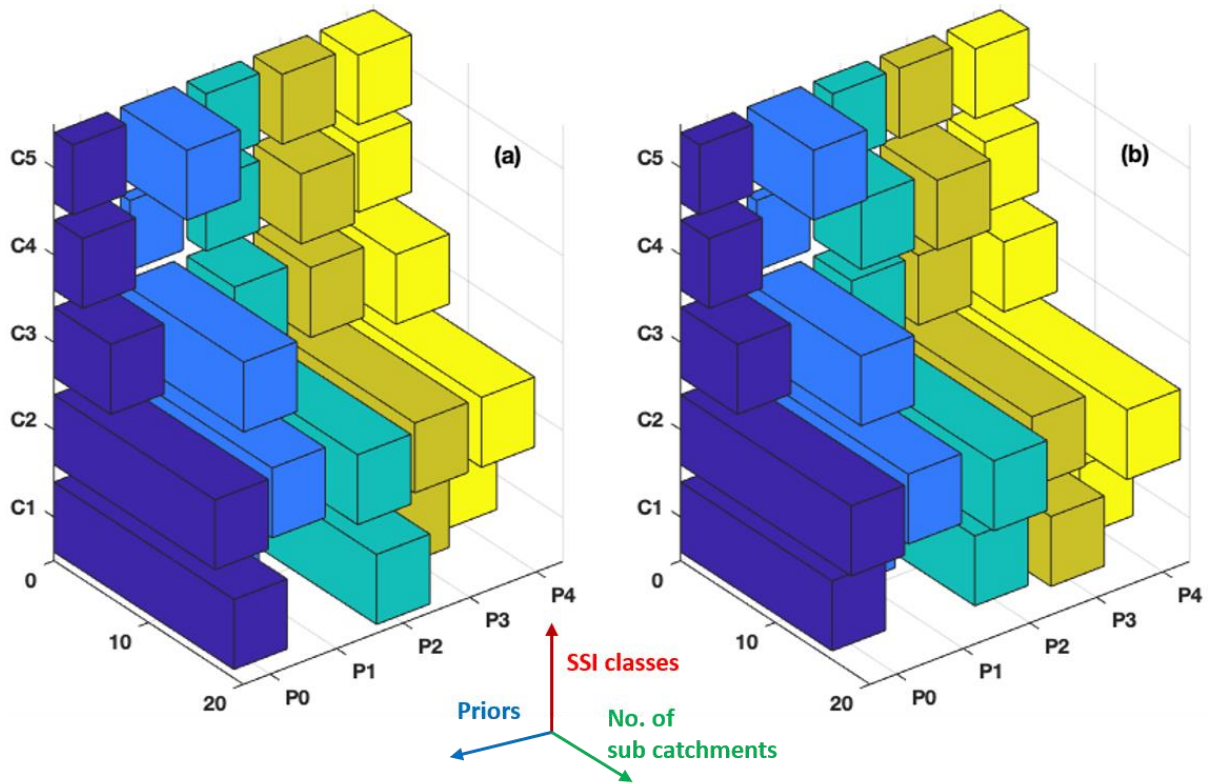


Figure 9 Distribution of numbers of sub-catchments based on respective SSI classes for each prior based Bayesian source apportionment model outputs in the two sampling time frames: (a) 2018-2019, and (b) 2021-2022.

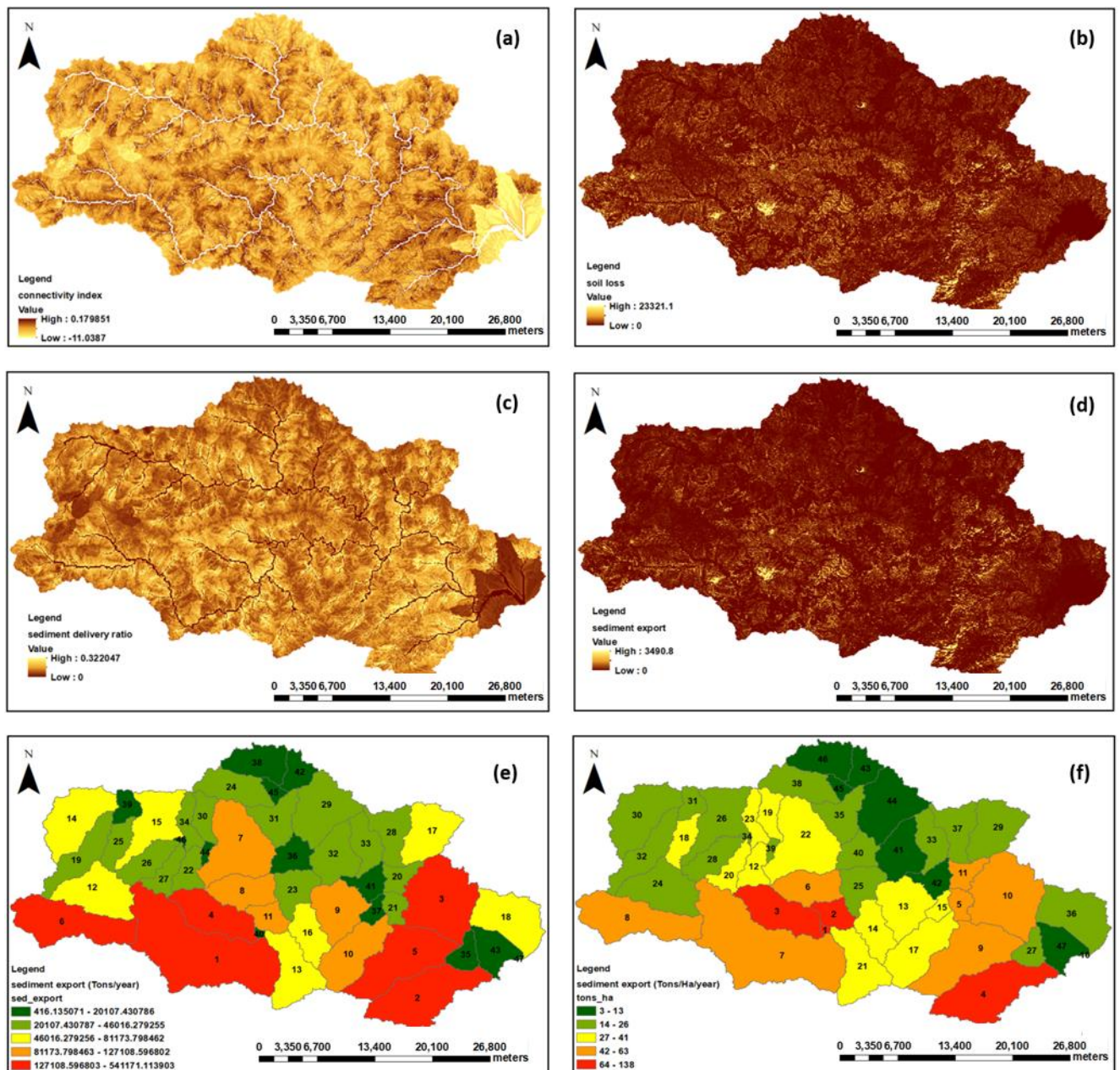


Figure 10 INVEST-SDR model outputs for the Konar study catchment, depicting the spatial variability in: (a) the connectivity index; (b) the annual soil loss (tons/year); (c) the sediment delivery ratio; (d) the annual sediment export (tons/year); (e) ranking and prioritization of the sub-catchments based on annual sediment export, and; (f) ranking and prioritization of the sub-catchments based on specific annual sediment yield. Note: the numbers on the sub-catchments (Figures e and f) represents their ranking based on the criteria.

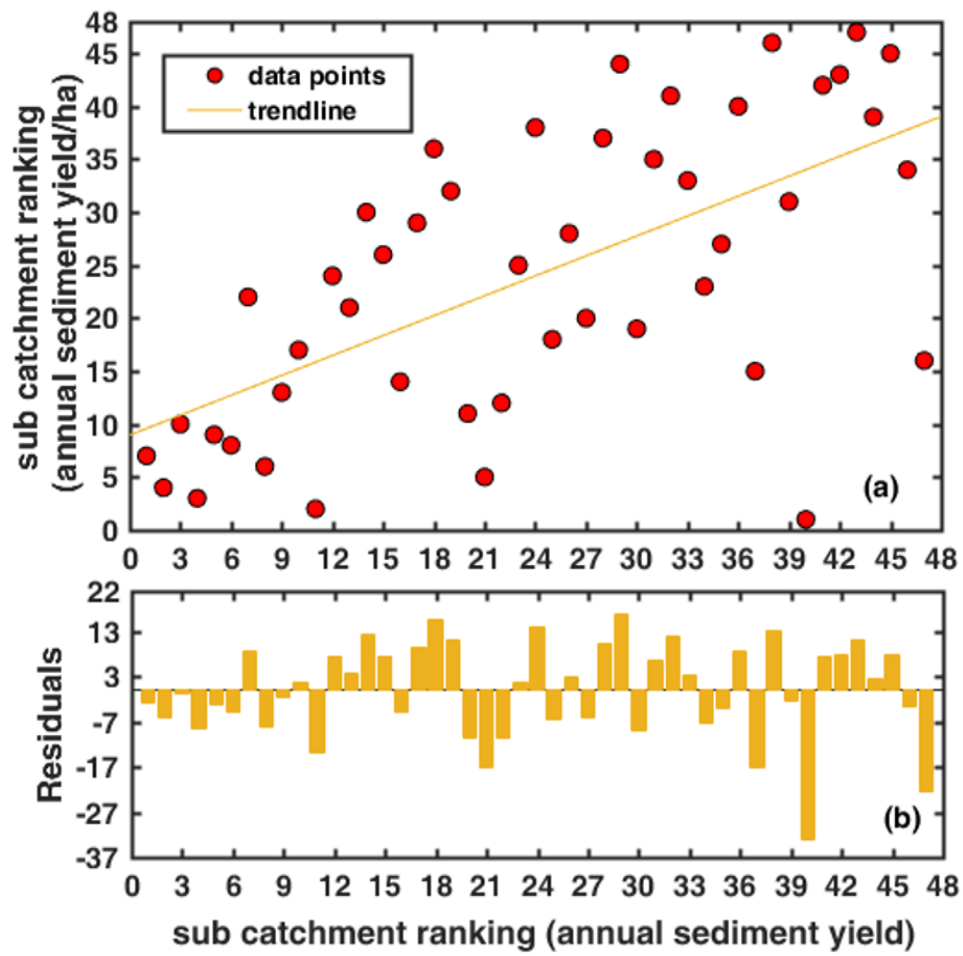


Figure 11 (a) Comparison between sub-catchment rankings based on annual sediment yield and annual specific sediment yield generated using the INVEST-SDR model. (b) Residuals of the ranking formats.

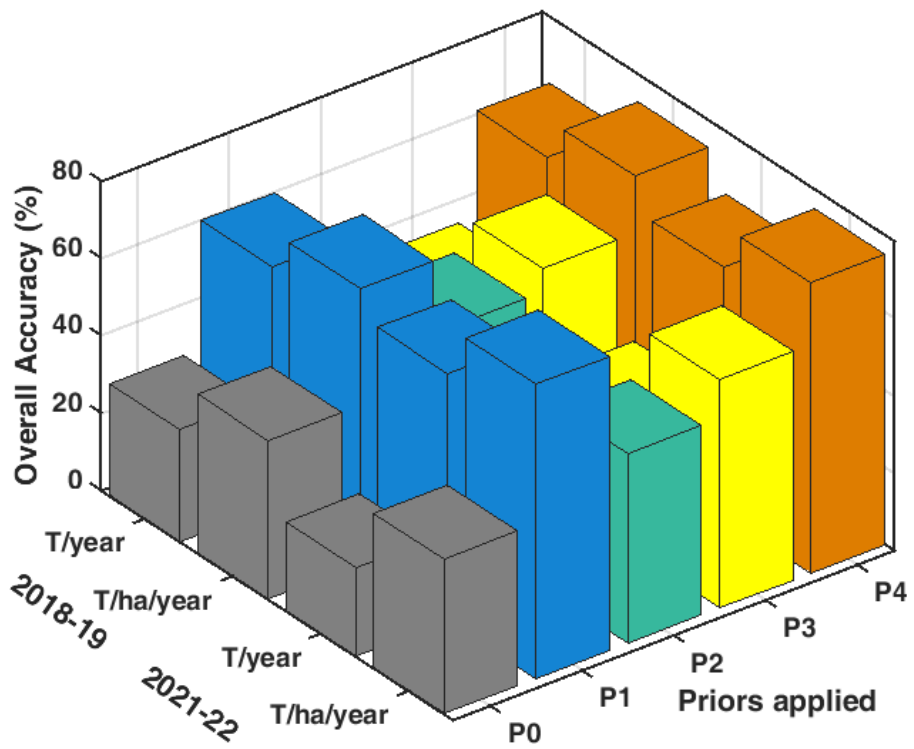


Figure 12 Overall accuracy (%) of the multiple prior based sediment fingerprinting SSI results compared with the INVEST-SDR predictions using confusion matrices.

The spatio-temporal dynamics of suspended sediment sources based on a novel indexing approach combining Bayesian geochemical fingerprinting with physically-based modelling

Arnab Das¹, Renji Remesan^{1*}, Adrian L. Collins²,

Ashok Kumar Gupta³

¹School of Water Resources, Indian Institute of Technology Kharagpur, India

²Net Zero and Resilient Farming, Rothamsted Research, North Wyke, Okehampton EX202SB, UK

³Department of Civil Engineering, Indian Institute of Technology Kharagpur, India

Supplementary Information

Tables

- **Table T1 Sampling details for source and reservoir target suspended sediment samples Jharkhand**
- **Table T2 Summary information on the geochemical properties of the source and target sediment samples**

Figures

- **Figure F1 FAO based soil map of the Konar River basin**
- **Figure F2 Distance factor for each sub-catchment used for developing the SSI**
- **Figure F3 INVEST-SDR model performance for sediment yield in the Konar river catchment**

Table T1 Sampling details for source and reservoir target suspended sediment samples Jharkhand

Period of sampling: 27 th June – 1 st August (2018)							
Tools used: Trowel, Polythene ziplock bags							
Steps	Explanation	Sites Information					Supportive references
Site selection	The sampling sites (n = 105) were selected on the basis of land use classes. The sampling sites were selected randomly so that they should be able to represent the heterogeneity of land use across the watershed.	Location Code	Locations	Land use classes present	Geographical Coordinates	Weather conditions during sampling	(Bahadori et al., 2019; Gaspar et al., 2019)
		1.1	Sultana	Hs, A, Ba	23 59 28/85 15 16	Cloudy	
		1.2	Banadag	FA	23 58 0/85 18 17	Cloudy	
		1.3	Hazaribagh town	FHs	23 58 33/85 15 48	Clear	
		1.4	Panchsheel colony	A	23 57 35/85 21 8	Clear	
Soil sample collection	All the soil samples were collected in zipped bags using a metallic trowel which was washed after every use to avoid contamination. The samples were collected from a depth of 0-5 cm .	1.5	Chehla, churchu road	F, Ba	23 55 49/85 25 25	Clear	(Nosrati and Collins, 2019)
		1.6	Rehda/ dumar	has	23 58 57/85 28 32	Clear	
		1.7	Chalchalia	F	23 55 18/85 31 29	Clear	
		1.8	Mangarpatta	FA, Ba	23 58 48/85 35 37	Clear	
		2.1	Sulmi	FHsA	24 4 56/85 19 12	Clear	
Composite Sampling	To make the analyses more affordable, composite samples were collected. Each composite sample consisted of a mixture of four to five sub- samples collected in a radius of 50 to 100 meters .	2.2	Jalima/bartua	FHsA	24 2 14/85 18 25	Clear	(Collins et al., 2010b)
		2.3	Moktama	FA, Ba	24 4 33/85 29 19	Clear	
		2.4	Vinod bhave university	FHs	24 1 16/ 85 22 0		
		2.5	Tepsa/saram	FHsA	24 3 49/85 24 24	Clear	
		2.6	Hazaribagh national park	FF, Ba	24 0 58/85 24 10	Clear	
		2.7	Barwa	HsA	24 4 5/85 26 52	Clear	

Processing	All source samples were oven dried for around 12 hours to remove the moisture content. Finally, after oven drying, the samples were passed through a 63µm sieve . The sieving undertaken to minimize contrasting grain sizes between the soil and target sediment samples.		2.8	Pundri/bandua	FF, Ba	24 1 51/85 29 16	Cloudy	(Tiecher et al., 2019)
			3.1	Bakra khurd/jagra	HsA	24 6 20/85 28 10	Cloudy	
			3.2	Darha	FHsA, Ba	24 6 36/85 30 51	Clear	
			3.3	Madhu kunj	FA	24 3 49/85 30 42	Clear	
			4.1	Khaira	FHsA, Ba	24 5 6/85 33 42	Clear	
			4.2	Basobar	FA	24 1 44/85 32 54	Clear	
			4.3	Hatwe	FA, Ba	24 0 47/85 36 23	Clear	
			5.1	Khamwa	FHsA, Ba	24 3 32/85 37 41	Clear	
			5.2	Siju	HsA	24 3 31/85 40 20	Clear	
			5.3	Holang	HsA, Ba	24 1 26/85 38 29	Drizzle	
			6.1	Kutse	FA, Ba	23 54 48/85 34 40	Clear	
			6.2	Hatwal	F, Ba	23 56 32/85 35 55	Clear	
			6.3	Alkhari khurd	FHsA	23 58 34/85 43 11	Clear	
			7.1	Belwara	F	24 0 52/85 40 48	Rainy	
			7.2	Hanuman temple near Belwara	FA	23 59 13/85 40 44	Rainy	
			7.3	Ambadih	FA, Ba	23 57 36/85 38 47	Clear	
			7.4	Gobindpur kalan	HsA, Ba	23 57 10/85 41 58	Rainy	
			7.5	Karidih	FHs, Ba	23 55 51/85 38 33	Clear	
7.6	Banda/bhitia	F	23 54 13/85 36 49	Clear				
Location	Sediment sampling Information					Supportive reference		
	Dates of sampling	Seasons						

Inflow point of the reservoir. (Magha [23 55 08/ 85 43 17])	July (2018)	Monsoon	All the target sediment samples were collected from a depth of 0-10 cm from the surface using High Density Polyethylene bottles. All bottle was washed prior to being used.	EPA (operating procedure) for surface water sampling & (Wang et al., 2019)
	August (2018)	Monsoon		
	October (2018)	Post monsoon		
	December(2018)	Post-monsoon		
	March (2019)	Pre-monsoon		
	June (2019)	Pre-Monsoon		
	July (2021)	Monsoon		
	August (2021)	Monsoon		
	October (2021)	Post monsoon		
	December(2021)	Post-monsoon		
	March (2022)	Pre-monsoon		
	June (2022)	Pre-Monsoon		

Table T2 Summary information on the geochemical properties of the source and target sediment samples

Soil properties (%)/ Land use details	Soil samples collected from the land use classes																			
	Agricultural lands				Forests				Barren lands				Human settlements				Sediment samples			
	Mean	Median	Min	Max	Mean	Median	Min	Max	Mean	Median	Min	Max	Mean	Median	Min	Max	Mean	Median	Min	Max
Fe	52.44	53.87	36.77	61.80	53.79	55.25	35.83	64.09	48.41	49.73	34.50	65.19	65.57	51.57	35.78	67.61	59.59	46.87	32.51	61.44
	52443	07585	66686	31957	37426	59103	10485	76394	43684	03193	08208	53114	76417	65574	16638	56874	36819	01965	6587	57559
K	26.62	24.12	18.44	43.78	27.31	24.74	17.97	45.41	24.58	22.27	17.30	46.18	33.29	30.16	23.14	56.31	30.25	27.41	21.03	51.17
	67432	4644	77141	65306	13833	49489	33773	21056	0245	0454	61156	97879	41347	55046	1998	55106	60449	29023	02907	67202
Ti	8.226	8.072	5.550	14.20	8.437	8.280	5.407	14.73	7.593	7.452	5.206	14.98	10.28	10.09	6.962	18.27	9.347	9.173	6.327	16.60
	15988	92072	15957	70847	67502	4957	45109	45227	90752	44613	69947	68514	60073	43967	4768	22682	40913	28303	15079	49237
Ca	6.789	6.049	3.507	13.47	6.963	6.204	3.417	13.97	6.267	5.584	3.290	14.21	8.489	7.563	4.400	17.32	7.714	6.873	3.998	15.74
	11047	1585	63235	32246	67547	69749	44235	34181	30792	22774	5698	27129	11774	88028	19941	8423	48575	6762	68121	72044
Zn	1.394	1.022	1.002	4.705	1.430	1.048	0.987	4.880	1.287	0.943	0.749	4.963	1.743	1.278	0.896	6.052	1.584	1.161	1.002	5.499
	53264	23172	3	56781	38956	51585	1	26201	35061	66427	15	8365	72649	20065	523	00846	61145	56484	58	76269
Mn	1.218	1.111	0.638	2.113	1.249	1.139	0.622	2.191	1.124	1.025	0.599	2.229	1.523	1.389	0.801	2.717	1.384	1.262	0.728	2.469
	50666	0612	72095	10978	83752	62936	29784	55898	85377	66642	19503	08942	62325	27321	2526	75028	59263	50203	1383	75557
Ba	1.185	1.117	0.693	1.666	1.215	1.146	0.675	1.728	1.094	1.031	0.650	1.758	1.482	1.397	0.870	2.143	1.346	1.270	0.790	1.948
	39249	83569	74696	90676	87189	57804	90899	79067	2847	92024	81587	39621	21721	74406	28076	87173	96489	19991	86764	24343
Zr	0.995	0.967	0.411	2.145	1.020	0.992	0.400	2.224	0.918	0.893	0.385	2.262	1.244	1.209	0.515	2.758	1.131	1.099	0.468	2.507
	39159	56093	07096	17571	9856	43935	5013	81535	88704	19541	63269	91532	6397	84019	67383	99149	06633	44227	61859	23351
Rb	0.258	0.211	0.145	0.662	0.265	0.217	0.142	0.687	0.238	0.195	0.136	0.698	0.323	0.264	0.182	0.852	0.294	0.240	0.166	0.774
	82955	89495	79645	51757	48471	3433	04766	11353	93624	60897	77414	88035	64101	95388	89644	08886	10876	77684	20714	33575
V	0.179	0.159	0.020	0.719	0.183	0.163	0.019	0.745	0.165	0.146	0.018	0.758	0.224	0.199	0.025	0.924	0.203	0.180	0.022	0.840
	36387	22419	08556	01064	97576	31824	56911	70391	57819	98642	84261	47409	27695	09426	19662	74674	81168	92691	89743	3636
Cr	0.148	0.155	0.051	0.228	0.152	0.159	0.050	0.237	0.137	0.143	0.048	0.241	0.185	0.193	0.064	0.293	0.168	0.176	0.058	0.267
	68678	07829	45774	5192	50989	06574	13464	00297	2589	15917	27339	06165	91826	91022	5519	90717	95322	21591	66154	08814
Sn	0.150	0.153	0.104	0.185	0.154	0.157	0.102	0.192	0.139	0.141	0.098	0.195	0.188	0.191	0.131	0.238	0.171	0.174	0.119	0.216
	69462	35216	83635	3196	56936	29523	14074	19959	11242	5657	34877	49101	42886	75186	51345	34653	23473	2545	51285	59741
Ni	0.103	0.105	0.059	0.129	0.106	0.108	0.058	0.134	0.095	0.097	0.055	0.136	0.129	0.132	0.074	0.166	0.117	0.120	0.067	0.151
	5817	88205	58265	6483	24504	60454	05063	4615	62054	74409	8955	76415	51877	39513	74431	74558	70018	31408	92389	53004
Sr	0.094	0.093	0.008	0.142	0.097	0.096	0.008	0.147	0.087	0.086	0.007	0.149	0.118	0.117	0.010	0.182	0.107	0.106	0.009	0.165
	78018	75682	49491	0046	21722	16754	27649	27652	4955	55079	96922	79863	51334	23372	65657	63748	69899	53614	68415	97181
Pb	0.047	0.042	0.023	0.097	0.048	0.043	0.023	0.100	0.043	0.039	0.022	0.102	0.058	0.053	0.029	0.124	0.053	0.048	0.027	0.113
	10794	77717	8035	06644	3192	87708	19145	67003	48728	48937	33047	394	90386	48866	86064	84081	52888	60782	13586	44909
Cu	0.045	0.043	0.031	0.084	0.046	0.044	0.031	0.087	0.041	0.039	0.029	0.089	0.056	0.054	0.039	0.108	0.051	0.049	0.036	0.098
	05262	19631	83113	47427	21103	30699	01267	61037	58993	87629	86132	1107	33389	01275	93101	64555	19342	08409	28731	73164
Ga	0.021	0.020	0.013	0.043	0.022	0.021	0.013	0.045	0.019	0.019	0.012	0.045	0.026	0.025	0.017	0.055	0.024	0.023	0.015	0.050
	46313	66514	68761	44121	015	1965	33567	05397	8135	07685	84058	82552	83755	83974	17062	87138	38862	48186	6038	77312
Sb	0.041	0.042	0.002	0.076	0.042	0.043	0.021	0.079	0.038	0.039	0.025	0.080	0.051	0.052	0.027	0.097	0.046	0.048	0.015	0.089
	3516	38063	57	17307	41485	47034	47	00099	17337	12331	871	35388	70612	99283	15	96906	98794	15723	736	02938

Ag	0.018	0.016	0.010	0.034	0.018	0.016	0.010	0.035	0.016	0.015	0.010	0.036	0.022	0.020	0.013	0.044	0.020	0.018	0.012	0.040
	08107	44419	71677	27788	54598	86701	44122	55045	69139	18031	05359	15925	60861	56184	44381	08608	54558	68557	21706	06322
As	0.007	0.007	0.004	0.013	0.007	0.007	0.002	0.013	0.006	0.007	0.001	0.014	0.008	0.009	0.004	0.017	0.007	0.008	0.004	0.015
	01544	70575	32	33029	19583	90389	79	82517	47624	1135	596	06193	77212	63529	597	14458	97167	75607	15	58014
Br	0.002	0.003	0.001	0.011	0.002	0.003	0.001	0.011	0.002	0.003	0.000	0.012	0.003	0.004	0.001	0.014	0.003	0.003	0.001	0.013
	91026	34191	27	40418	98509	42784	87	82756	68658	08506	982	03011	639	17873	93	66735	30694	79742	058	32895

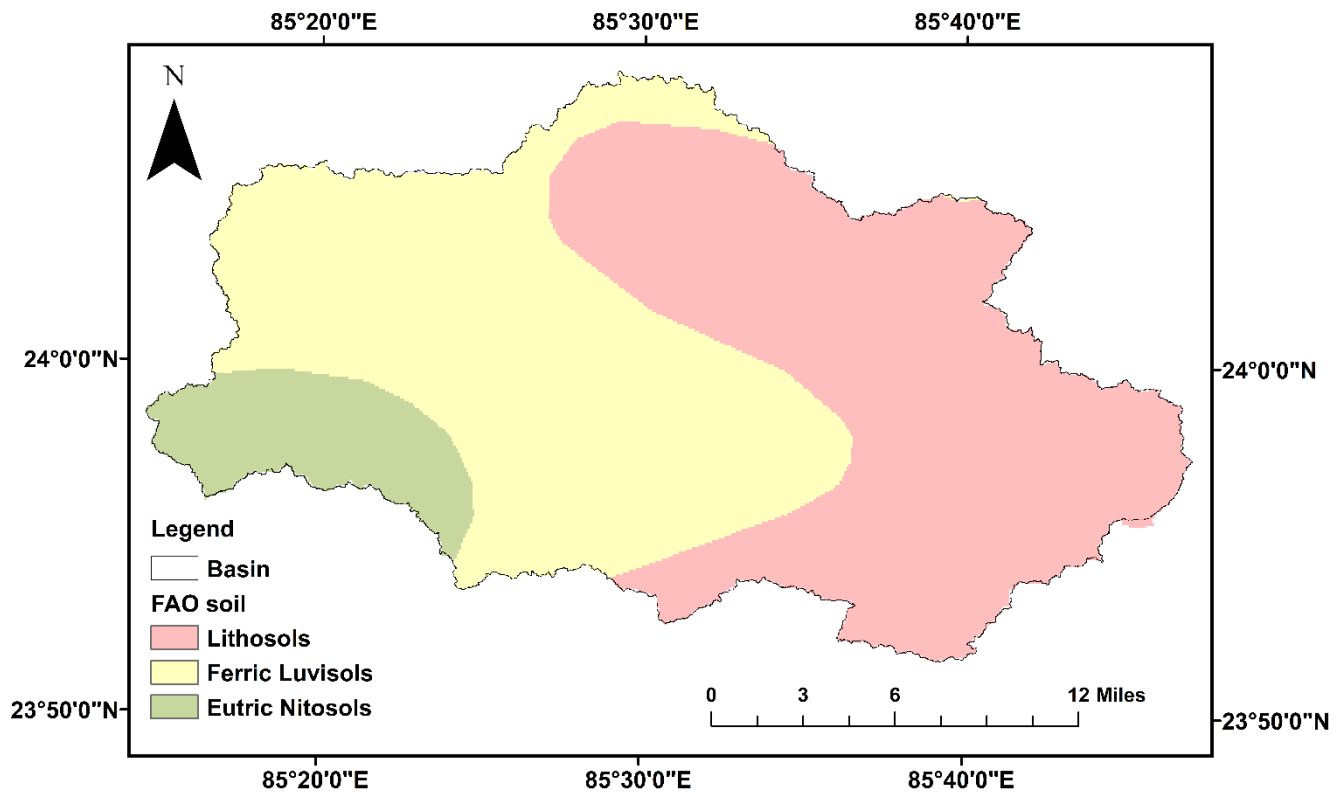


Figure F1 FAO based soil map of the Konar River basin

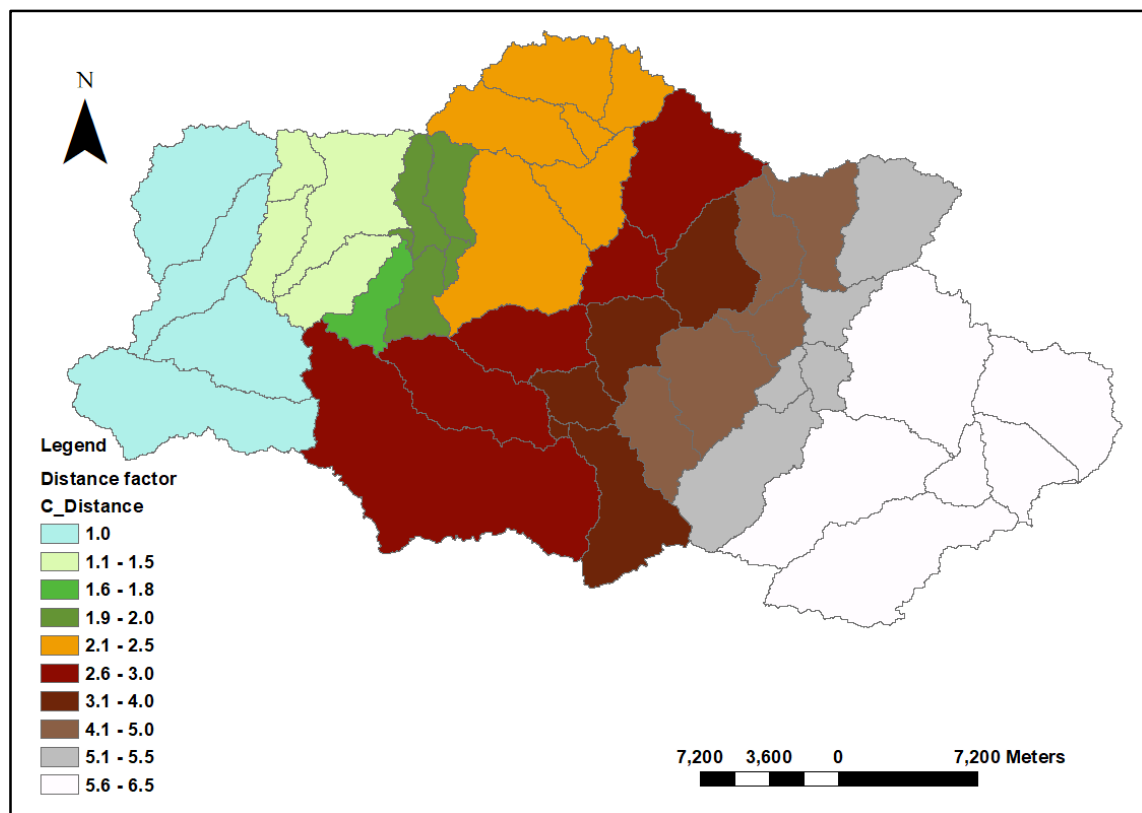


Figure F2 Distance factor for each sub-catchment used for developing the SSI

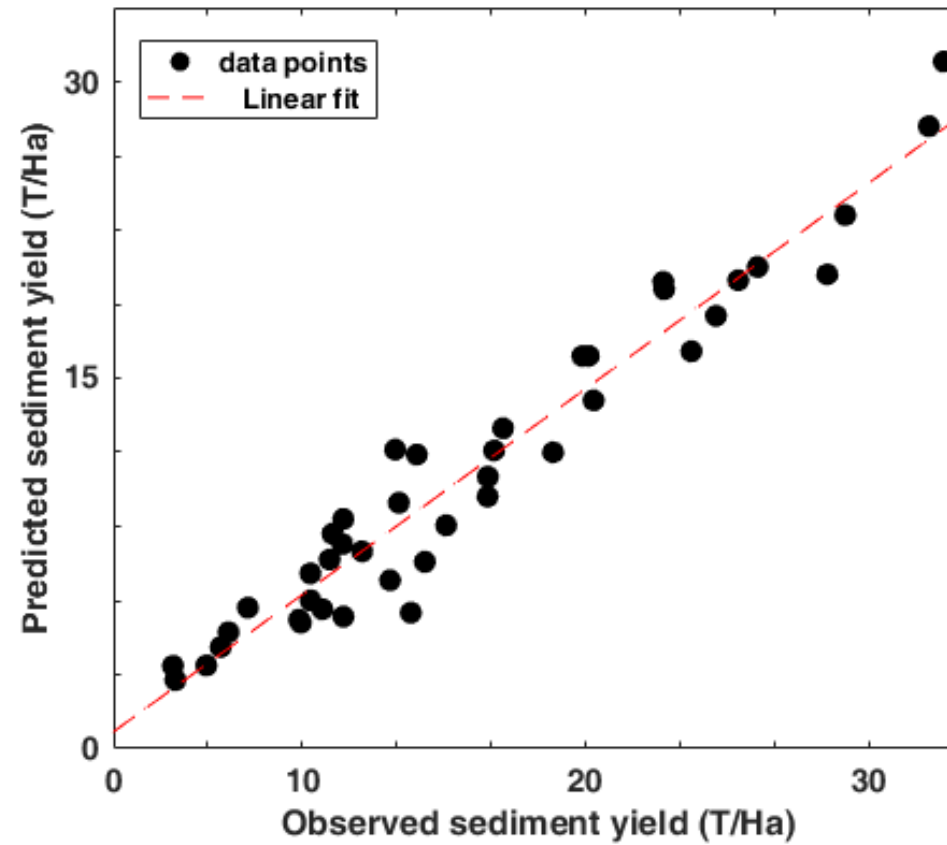


Figure F3 INVEST-SDR model performance for sediment yield in the Konar river catchment

Arnab Das: Modelling, Data curation, Writing- Original draft preparation, Visualization

Renji Remesan: Supervision, Conceptualization, Methodology, Writing

Adrian L. Collins: Supervision, correction and second draft preparation, funding

Ashok Kumar Gupta: Supervision, Validation, Writing- Reviewing and Editing,
All authors reviewed the results and approved the final version of the manuscript

Declaration of interests

The authors declare that they have no known competing financial interests or personal relationships that could have appeared to influence the work reported in this paper.